

HANNES KEERNIK

Estimating methods and variability
of atmospheric humidity over
the Baltic Region and the Arctic



HANNES KEERNIK

Estimating methods and variability
of atmospheric humidity over
the Baltic Region and the Arctic



This study was carried out at Tartu Observatory and at the Institute of Physics, University of Tartu.

The dissertation was admitted on March 27, 2015, in partial fulfilment of the requirements for the degree of Doctor of Philosophy in physics (environmental physics), and was allowed for defence by the Council of the Institute of Physics, University of Tartu.

Supervisors: Assoc. Prof. Hanno Ohvril,
Institute of Physics, University of Tartu, Estonia
PhD Erko Jakobson,
Institute of Physics, University of Tartu, Estonia

Opponents: Prof. Irina Melnikova, Saint Petersburg State University
Prof. Sirje Keevallik, Tallinn University of Technology

Defence: June 5, 2015, at the University of Tartu, Estonia

These studies were supported by European Social Fund's Doctoral Studies and Internationalisation Programme DoRa. Programme DoRa is carried out by Archimedes Foundation.



ISSN 1406-0310
ISBN 978-9949-32-802-4 (print)
ISBN 978-9949-32-803-1 (pdf)

Copyright: Hannes Keernik, 2015

University of Tartu Press
www.tyk.ee

CONTENTS

LIST OF ORIGINAL PUBLICATIONS	6
OTHER PUBLICATIONS	7
ACRONYMS	8
1. INTRODUCTION.....	9
2. METHODS AND DATA.....	12
2.1. Radiosonde.....	12
2.1.1. Temperature-dependence corrections	15
2.1.2. Time-lag correction.....	16
2.2. GPS	18
2.3. AERONET	21
2.4. Regional and global models	22
2.5. Data processing.....	23
3. LONG-TERM VARIATIONS AND TRENDS.....	28
3.1. Impact of the radiosonde corrections on humidity	28
3.2. Yearly trends	30
3.3. Monthly trends	34
4. DIURNAL CYCLE.....	38
4.1. Diurnal cycle depending on the underlying surface and sea/land breeze	38
4.2. Layers responsible for diurnal cycle	40
5. INTERCOMPARISONS BETWEEN TECHNIQUES AND MODELS...	42
5.1. Intercomparisons in Estonia	42
5.1.1. The campaign from 22 June to 6 November 2008 at Tõravere...	42
5.1.2. The campaign from 9 to 12 August 2010 at Tõravere	44
5.2. Validation of reanalyses over the Arctic.....	46
6. CONCLUSIONS	50
6.1. The main findings	50
6.2. Pathways for further research.....	51
SUMMARY IN ESTONIAN	53
REFERENCES	56
ACKNOWLEDGEMENTS	61
PUBLICATIONS	63
CURRICULUM VITAE	103
ELULOOKIRJELDUS.....	104

LIST OF ORIGINAL PUBLICATIONS

This thesis contains the research published in the following papers (full texts included at the end of the thesis):

- I Keernik, H., Ohvri, H., Jakobson, E., Rannat, K., Luhamaa, A. (2014). Column water vapour: an intertechnique comparison of estimation methods in Estonia. *Proc. Estonian Acad. Sci.*, **63**, 1, 37–47.
- II Jakobson, E., Keernik, H., Luhamaa, A., Ohvri, H. (2014). Diurnal variability of water vapour in the Baltic Sea region according to NCEP-CFSR and BaltAn65+ reanalyses. *Oceanol.*, **56**, 2, 191–204.
- III Jakobson, E., Vihma, T., Palo, P., Jakobson, L., Keernik, H., Jaagus, J. (2012). Validation of atmospheric reanalyses over the central Arctic Ocean. *Geophys. Res. Lett.*, **39**(L10802), 1–6.

Author's contribution

The papers which form the basis for the major part of the thesis are the result of collective work and contain important contributions from all the co-authors. The author's contribution to the publications is indicated as follows:

- I Performed most calculations, prepared the full text of the paper and communicated with the Editorial Board.
- II Wrote the relevant text for introduction as well as materials and methods, interpreted the results, reviewed the manuscript.
- III Investigated the sources of input data and its processing schemes in different reanalyses, wrote the relevant text, reviewed the manuscript.

OTHER PUBLICATIONS

- Keernik, H., Ohvril, H., Jakobson, E., Rannat, K., Luhamaa, A. (2011). Õhusamba niiskussisalduse erinevate määramisviiside võrdlus. *Publicationes Instituti Geographici Universitatis Tartuensis*, 109, 179–193.
- Keernik, H., Jakobson, E., Ohvril, H. (2013). Trends in tropospheric humidity and temperature over Estonia and Finland derived from radiosonde measurements. In: Conference Proceedings: Seventh Study Conference on BALTEX, Borgholm, Island of Öland, Sweden, 10 to 14 June 2013. (Eds.) Marcus Reckermann and Silke Köppen. International BALTEX Secretariat: 69–70.
- Keernik, H., Ohvril, H., Jakobson, E., Rannat, K., Luhamaa, A. (2013). Column water vapour: An intertechnique comparison of estimation methods in Estonia. In: Geophysical Research Abstracts: European Geosciences Union–General Assembly, Vienna, Austria.
- Jakobson, E., Keernik, H., Luhamaa, A., Ohvril, H. (2013). Diurnal variability of water vapour in the Baltic Sea region according to NCEP-CFSR and BaltAn65+ reanalyses. In: Conference Proceedings: Seventh Study Conference on BALTEX, Borgholm, Island of Öland, Sweden, 10 to 14 June 2013. (Eds.) Marcus Reckermann and Silke Köppen. International BALTEX Secretariat: 67–68.

ACRONYMS

AERONET	Aerosol Robotic Network
GPS	Global Positioning System
HIRLAM	High Resolution Limited Area Model
MBD	mean bias difference
NAO	North Atlantic Oscillation
PW	precipitable water
RH	relative humidity
RH _{corr}	Vaisala RS80-A corrected relative humidity derived from a temperature-dependence or time-lag correction
RH _{meas}	relative humidity measured by Vaisala RS80-A
RMSD	root-mean-square difference
SH	specific humidity
STD	slant total delay
TD	temperature-dependence
TD-M	temperature-dependence correction for Vaisala RS80-A proposed by Miloshevich <i>et al.</i> (2001)
TD-L	temperature-dependence correction for Vaisala RS80-A proposed by Leiterer <i>et al.</i> (2005)
TL	time-lag
TL-M	time-lag correction for Vaisala RS80-A proposed by Miloshevich <i>et al.</i> (2004)
ZTD	zenith total delay
ZHD	zenith hydrostatic delay
ZWD	zenith wet delay

I. INTRODUCTION

Atmospheric water vapour, although providing the largest greenhouse effect on the Earth's climate, is still poorly measured and understood. In current meteorological practice, a significant challenge in measurements is related to estimation of its spatial and temporal distribution (Bengtsson *et al.*, 2003; Kämpfer, 2013). To overcome this problem, several new techniques have been increasingly available during the last few decades, e.g. Global Positioning System (GPS) (Bevis *et al.*, 1992) and satellite meteorology (Schlüssel and Emery, 1990; Gao and Kaufmann, 2003), which are now used along with more traditional methods as radiosonde. In addition, databases of numerical weather prediction and reanalyses have proved to be useful tools in estimating the state of the atmosphere, especially in areas, where the scarcity of observing systems restricts investigation (e.g. seas, large lakes, polar regions). However, despite of several estimation techniques for column water vapour amount, no method or model is yet identified as the most accurate or the reference one. This drives a necessity to continuously perform intercomparisons, which help to evaluate strengths and weaknesses, accuracy and biases of different methods. An overview of previous intercomparisons including four methods available also in Estonia is presented in the appended publication I.

On the other hand, regarding the factors controlling vertical profile of water vapour, its column amount and the atmospheric mechanisms which are influenced by them, work to date has not led to a universally accepted picture (Sherwood *et al.*, 2010). As water vapour is active chemically, radiatively and physically, its distribution influences precipitation, clouds, chemical reactions, incoming solar radiation, outgoing heat, etc. Like other natural components of the Earth's atmosphere, variations in the water vapour amount are normal, but in order to understand, associate and forecast atmospheric processes, determining their extent is critical. This is especially important in climate research, while water vapour provides the largest positive feedback in model projections of climate change (Held and Soden, 2000; Solomon *et al.*, 2007).

Only a few studies have focused on investigation of tropospheric temperature and water vapour distribution changes over Europe during the last few decades (Gaffen *et al.*, 1992; Ross and Elliot, 2001; Trenberth *et al.*, 2005; Durre *et al.*, 2009; McCarthy *et al.*, 2009; Mattar *et al.*, 2011). Most of them have evidenced a small increase in those characteristics. In addition, some authors have reported the same tendency at surface level (Dai, 2006; Willett *et al.*, 2008). Regarding the tropospheric water vapour, studies have mainly dealt with originally homogeneous radiosonde datasets, avoiding using the data from stations with changes in sonde types, or have abandoned the data above 500 hPa where large errors in humidity measurements occur, rather than correcting humidity profiles.

Considering the entire vertical cross-section of the atmosphere, the water vapour is often quantified as the column integrated water vapour or simply,

precipitable water (PW), equal to thickness of the layer of liquid water if all water vapour per unit area were condensed. Its SI-unit, kg/m^2 , is equivalent to mm. In this thesis, the main focus is on variability of PW as well as on its directly-related characteristic, specific humidity (SH).

Besides focusing on problems of vertical distribution of temperature and humidity in the entire tropospheric column of the Baltic Sea Region, the dissertation deals with accuracy of reanalyses-based temperature and humidity in the lowermost atmosphere (1 km) in the Central Arctic Ocean. It should be noted that the Arctic, because of its growing strategic importance, is a region of special interests for the EU: “Rapid climate change, a major concern and cause of fundamental changes in the Arctic, combined with increased prospects for economic development in the Arctic region call for the EU to engage actively with Arctic partners to assist in addressing the challenge of sustainable development in a prudent and responsible manner” (EU FAC, 2014).

In the Arctic, from a physical point of view, there are two major contributing factors which may further speed up the entire global warming process. First, as the atmosphere warms, it holds more water vapour. Secondly, the Arctic ice firmly separates the ocean and the atmosphere like a lid. The loss of sea-ice in the Arctic means that more water vapour is being pumped up into the atmosphere. The process is called as *the Arctic amplification* of global warming (EM, 2012; Law, 2014).

Because of drifting ice cover in the Arctic, creation of permanent observational stations (like in the Antarctic) is impossible. This difficulty should be overcome by use of satellite observations, climate models and reanalyses databases. However, for validation of remote and interpolation methods, reference profiles obtained by direct atmospheric soundings are necessary. In this dissertation, a dataset of reference profiles obtained using tethered sonde soundings from the ice station Tara (France) during a period from April to August in 2007 was available (Section 5.2). It should be noted that one of the supervisors of this dissertation, Erko Jakobson, performed these soundings working on board of R/V Tara.

The aims of the current thesis are as follows:

- investigate long-term variability and trends in vertical humidity profiles, based on homogenized humidity datasets from radiosonde stations in Estonia and Finland;
- investigate diurnal cycle of PW in the Baltic Region at summer and determine the layers responsible for changes within 24-h period, based on datasets produced for period of 1979–2005 by two reanalyses, NCEP-CFSR and BaltAn65+;
- estimate the accuracy of different PW methods available in Estonia and suggest an alternative method to radiosonde, which has been historically set as a reference;

- validate global reanalyses temperature and humidity profiles against direct tethersonde soundings for the lowermost Arctic's atmosphere.

The thesis is structured as follows. Chapter 2 introduces three PW measurement techniques: radiosonde, GPS and AERONET. All measurements made by these techniques are subject to error sources. Thus, PW retrievals are explained together with uncertainty estimates. In addition, an overview of models and reanalyses is given. This chapter also includes comments on how the experiments and calculations were carried out.

Long-term variation of atmospheric humidity and its trends over Estonia and Finland derived from homogenized radiosonde data are presented in Chapter 3.

Diurnal cycle of PW, investigated using datasets from NCEP-CFSR and BaltAn65+ reanalyses during the period 1979–2005 over the Baltic Region, is discussed in Chapter 4. The changes are analysed during 6-hour increments and the influence of different layers on the diurnal variation of PW is determined.

Chapter 5 focuses on intercomparisons between radiosonde, GPS, AERONET and a regional model HIRLAM made for Estonia as well as between five reanalyses investigated in the Arctic.

Finally, the conclusions are presented in Chapter 6.

2. METHODS AND DATA

2.1. Radiosonde

Radiosonde has for decades been a traditional worldwide instrument for evaluation of tropospheric humidity and temperature profiles. In studying heterogeneous radiosonde time series which include measurements carried out by different radiosonde types, corrections are needed to improve the accuracy and eliminate biases. Vaisala Oy is a Finnish company, that develops radiosondes which have been proved to be reliable and these are most widely used in Global Climate Observing System (GCOS) network (GCOS, 2010). Its commercial production dates back to 1936. The most remarkable change in Vaisala's radiosonde development took place in 1981 when hairhygrometers were replaced with Humicap technology. Until that time, "reliable humidity measurement was an unresolved challenge" (Vaisala, 2012). Therefore, the time series measured by these two technologies should be separated for trend calculations. Humicap sensors were first integrated into RS80 radiosondes, later into RS90 and RS92 radiosondes. These three types of sondes have been also used in Harku, Estonia since 1993, when the sondes manufactured in the former USSR were replaced by the Vaisala products (Keevallik and Krabbi, 2011). In Finland these have been used since 1982.

The errors of Vaisala radiosondes using Humicap technology are relatively well-known, thereby offering opportunity to develop corrections to eliminate them. Sonde RS80 equipped with an A-Humicap sensor (RS80-A), which is the only sensor type of RS80 used in all of the stations investigated, suffers from several types of errors:

- inadequate temperature-dependence (TD) correction derived from a deficient calibration model, resulting in significant dry bias at temperatures below -20°C (Miloshevich *et al.*, 2001; Wang *et al.*, 2002; Leiterer *et al.*, 2005);
- sensor time-lag (TL) derived from slow response time with decreasing temperature, resulting in smoothing of the relative humidity (RH) profile and bias depending on the sign of the vertical RH-gradient;
- chemical contamination derived from packaging material used in production before June 2000, resulting in dry bias of about 2% throughout the troposphere, depending on the storing time and storage conditions (Wang *et al.*, 2002);
- daytime radiation dry bias, derived from heating of the sensor arm (Cole and Miller, 1995; Wang *et al.*, 2002);
- condensation and sublimation, resulting in wet bias and slow response.

First of them is the dominant systematic error in A-type Humicap measurements and results in bigger dry bias than newer versions of Vaisala sondes (Miloshevich *et al.*, 2001; Wang and Zhang, 2008; Smit *et al.*, 2013). There are two corrections, which have been used to eliminate this error. First,

Miloshevich *et al.* (2001) proposed the multiplicative RH correction factor of about 1.1 at $-35\text{ }^{\circ}\text{C}$, 1.4 at $-50\text{ }^{\circ}\text{C}$, 1.8 at $-60\text{ }^{\circ}\text{C}$ and 2.5 at $-70\text{ }^{\circ}\text{C}$. Secondly, Leiterer *et al.* (1997; 1998; 2005) developed a correction method using modified RS90 sonde as a reference to carry out about 70 simultaneous soundings. The TL correction used in this work was developed by Miloshevich *et al.* (2004) by examining seven RS80-A sensors over the temperature range $+25\text{ }^{\circ}\text{C}$ to $-60\text{ }^{\circ}\text{C}$ in rapidly changing humidity conditions. Regarding TL correction, its application is more limited due to the fact, that time resolution of measurements made during the ascent should be $\leq 10\text{ s}$. This means that original profiles without averaging should be used and data archived only at “mandatory and significant levels” can not be corrected for TL error. The author of this thesis tested the TL correction for data collected at Harku in 1998, when above-mentioned condition was met. The correction for eliminating chemical contamination takes into account the sonde’s age and storage conditions (Wang *et al.*, 2002). Due to the fact, that the author had no such information, this was not applied. There are two correction algorithms to eliminate daytime radiation bias of RS80-A (Cole and Miller, 1995; Wang *et al.*, 2002). However, because this study was carried out only for 00 UTC (and 06 UTC for Jyväskylä since 1997), the problem did not affect the measurements used.

Introducing the RS90 and RS92 sondes with a heated H-polymer twin sensor design, the errors related to sensor icing and chemical contamination were minimized (Paukkunen, 1995; Van Baelen *et al.*, 2005). In addition, due to the smaller sensor size on both of the sondes, TL was effectively reduced (Miloshevich *et al.*, 2004) and new calibration models introduced in 2001 for RS90 (Paukkunen, 1998; Paukkunen *et al.*, 2001) and in 2004 for RS92 have considerably improved the accuracy compared to RS80-A (Vömel *et al.*, 2007a). Still, a daytime radiation bias is a problem, which magnitude is even larger than it was in case of RS80-A (Van Baelen *et al.*, 2005; Miloshevich *et al.*, 2006; Vömel *et al.*, 2007a; Cady-Pereira *et al.*, 2008; Wang and Zhang, 2008), because RS90 and RS92 do not have a aluminized protective shield to prevent the impact of solar radiation.

Retrieval of the radiosonde-estimated precipitable water (PW) involves integrating specific humidity (SH) values over all pressure levels, p :

$$\text{PW} = \frac{1}{g} \int_{p_0}^{p_1} \text{SH}(p) \cdot \delta p \approx \frac{1}{g} \sum_i \text{SH}(p_i) \cdot \Delta p_i, \quad (2.1)$$

where g denotes acceleration due to the gravity and SH (g/kg) is calculated as follows:

$$\text{SH} = 622 \frac{e}{p - 0.378e}, \quad (2.2)$$

where p is barometric pressure and e is water vapour pressure, both in hPa. The latter is given according to the Magnus type equation (Aruksaar *et al.*, 1964):

$$e = 0.061078 \cdot 10^{\frac{7.567 \cdot T - 2066.92805}{T - 33.45}} \cdot \text{RH}, \quad (2.3)$$

where T denotes temperature (K). It has been shown that the relative uncertainty in PW is equal to the relative uncertainty in SH (Jakobson, 2009):

$$\frac{u(\text{PW})}{\text{PW}} \approx \frac{u(\text{SH}(p_i))}{\text{SH}(p_i)}, \quad (2.4)$$

where uncertainty in SH, in turn, is given as:

$$u(\text{SH}) = \sqrt{\left(u(e) \cdot \frac{\partial}{\partial e} \text{SH}(e, p)\right)^2 + \left(u(p) \cdot \frac{\partial}{\partial p} \text{SH}(e, p)\right)^2} \quad (2.5)$$

and uncertainty in e is:

$$u(e) = \sqrt{\left(u(T) \cdot \frac{\partial}{\partial T} e(T, \text{RH})\right)^2 + \left(u(\text{RH}) \cdot \frac{\partial}{\partial \text{RH}} e(T, \text{RH})\right)^2}. \quad (2.6)$$

According to Equation (2.4) and relying on technical information provided by manufacturers, relative standard uncertainty in PW estimated by Vaisala RS80-A, RS90 and RS92 is about 4%. On the other hand, GRAW DFM-06 (Germany) sondes, used in comparisons carried out in Estonia (see Chapter 5), are found to be more accurate with relative standard uncertainty in PW only 2% (GRAW, 2014).



Figure 1. Climatologist Ain Kallis (left) is holding the GRAW DFM-06 unit, while the balloon is being inflated. The picture was taken during the experiment held in August 2010 at Tõravere, Estonia.

2.1.1. Temperature-dependence corrections

The Vaisala RS80-A humidity datasets from four radiosonde stations in Estonia and Finland were recalculated using two TD correction methods. The correction proposed by Miloshevich *et al.* (2001) is based on the test of 16 sensors in calibration chamber at Vaisala. The RH correction factor, $F(T)$, for TD error can be found as follows:

$$F(t) = \frac{RH_i(t)}{RH_i(t) - C(t)}, \quad (2.7)$$

where t is temperature (in degrees Celsius), RH_i is relative humidity (with respect to water) on ice saturation and is calculated using Wexler-Hyland formulations (Wexler, 1976; Hyland and Wexler, 1983):

$$RH_i(t) = \frac{e_i(t)}{e_w(t)} \times 100\%, \quad (2.8)$$

where e_i and e_w are saturation vapour pressures over ice and liquid water, respectively. The coefficients of the fifth-order polynomial, $C(t)$, are: $a_0 = 0.3475$, $a_1 = 2.83 \times 10^{-2}$, $a_2 = 4.209 \times 10^{-4}$, $a_3 = -1.4894 \times 10^{-4}$, $a_4 = 6.4325 \times 10^{-7}$, and $a_5 = 2.1677 \times 10^{-8}$.

The correction proposed by Leiterer *et al.* (2005) is calculated as follows:

$$\begin{aligned} \text{RH}_{\text{corr,w}} = & \text{RH}_{\text{meas,w}} + \left[\frac{\Delta_1 \text{RH}_{\text{G,w}}(\text{RH}) \times \text{RH}_{\text{meas,w}}}{100\%} \right] + \\ & + \Delta_2 \text{RH}_w(t) \left[\frac{\text{RH}_{\text{meas,w}} + \frac{\Delta_1 \text{RH}_{\text{G,w}}(\text{RH}) \times \text{RH}_{\text{meas,w}}}{100\%}}{\text{RH}_i(t) - \Delta_2 \text{RH}_w(t)} \right], \end{aligned} \quad (2.9)$$

where RH_{meas} denotes RH measured by RS80-A; $\Delta_1 \text{RH}_{\text{G,w}}(\text{RH})$ is a mean dry bias correction for historical RS80-A data, it equals to 5.6% for sonde produced before April 2000 and 2% for sonde produced after April 2000; $\Delta_2 \text{RH}_w(t)$ is an additional TD correction function, $\Delta_2 \text{RH}_w(t) = 0$ for temperatures $> -15^\circ \text{C}$, otherwise $\Delta_2 \text{RH}_w(t) = At^2 + Bt + C$, with temperature t ($^\circ \text{C}$) and the coefficients $A = 0.005$, $B = 0.112$, $C = 0.404$; RH (with respect to water) on ice saturation is calculated instead of Wexler-Hyland equations using formulas given by Sonntag (1994). Since there was no information about the date of the sonde's production available, $\Delta_1 \text{RH}_{\text{G,w}}(\text{RH})$ value 5.6% was used before 1 January 2001, after that date 2% was used.

2.1.2. Time-lag correction

The time response of the sensor determines whether humidity profile has high or low level of detail. It can be described by the time constant, τ , which is the time required for the sensor to respond to 63% of an instantaneous change in the ambient humidity. In the correction algorithm (Miloshevich *et al.*, 2004), it is given by:

$$\tau(t) = 10^{P(t)} \times F(t), \quad (2.10)$$

where $P(t)$ is a fourth-order polynomial fit at temperature t (in degrees Celsius) with the following coefficients: $a_0 = -1.7542 \times 10^{-1}$, $a_1 = -2.97467 \times 10^{-2}$, $a_2 = 1.71521 \times 10^{-4}$, $a_3 = 8.21223 \times 10^{-7}$, $a_4 = -1.44814 \times 10^{-8}$; and $F(t)$ is an adjustment factor to decrease the time constant values by one standard deviation to avoid overcorrection for some radiosondes. Vaisala radiosonde humidity data is corrected for TL error by applying the following equation to each time step in a humidity profile:

$$\text{RH}_{\text{corr}} = \frac{\text{RH}_{\text{meas}}(T_f) - [\text{RH}_{\text{meas}}(T_0)X]}{1 - X}, \quad (2.11)$$

where $X \equiv e^{-\Delta T/\tau}$; ΔT is sample spacing (10 s for the data used in this thesis); RH_{corr} is the ambient (corrected) humidity required to drive the measured change during the time step; $\text{RH}_{\text{meas}}(T_0)$ and $\text{RH}_{\text{meas}}(T_f)$ denote the measured humidity at the beginning and at the end of the time step, respectively.

However, direct application of Equation (2.11) fails because RH data are usually recorded with the resolution of 1%. Archiving data this way produces profiles which resemble stairs: RH constant time steps are followed by an abrupt change of 1% RH during a single time step. Consequently, it produces large spikes in RH_{corr} , because the ambient humidity must be very different from RH_{meas} to cause such an abrupt change in RH_{corr} when temperature is very low and τ is relatively large. Thus, there is a necessity to work with smoothed profiles, while the amount of total smoothing is less than the resolution of the measurements. This is achieved by four steps:

- a skeleton profile is constructed by assigning a single point in the centre of the constant RH period and additional points near the end of the constant period that is at least 7 timesteps (70 s) long;
- the skeleton profile is smoothed so the changes in the curvature are minimized, adjusting points added within its specified tolerance range. For peaks wider than 7 timesteps (if these are not in the stratosphere), the tolerance value of the middle point ranges from ± 0.15 to $\pm 0.5\%$, depending on the sensor time constant which is from 0.1 to 220 s, respectively, while for endpoints of long constant period $\pm 0.5\%$ is always used. For peaks narrower than 7 timesteps, the tolerance value from ± 0.3 to $\pm 0.5\%$ (time constant from 0.1 to 220 s, respectively) is used. For peaks in the stratosphere, whether narrow or wide, the tolerance value is always $\pm 0.5\%$;
- RH_{meas} profile is recalculated using Equation (2.11) and smoothed again with a tolerance of $\pm 0.15\%$;
- going from sparse “skeleton profile” to a spline fit for the original 10 s time series, smoother results are achieved with two intermediate steps by which another data point is added linearly between the existing smoothed sparse data points and smoothed again with a tolerance value of $\pm 0.05\%$. The reason this will give a smoother result than going directly to the full time series is that there is a highly non-linear relationship between the measured and corrected RH profiles;
- spline interpolation is used to retrieve the final RH_{corr} profile.

These three correction methods for TD and TL errors have been tested by Suortti *et al.* (2008) during the one-month experiment held in Northern Finland at Sodankylä in February 2004. Regarding TD correction, it was concluded, that the method proposed by Leiterer *et al.* (2005) was the best available, removing

the dry bias throughout lower and mid troposphere. For temperatures below $-30\text{ }^{\circ}\text{C}$, the dry bias of 5% was still notable in the upper troposphere. Results showed that the TD correction method by Miloshevich *et al.* (2001) tends to overcorrect humidity at temperatures below $-50\text{ }^{\circ}\text{C}$ and is ineffective above $-30\text{ }^{\circ}\text{C}$. The TL correction had no major impact on the yearly RH value.

However, the author of this thesis is not aware of any study, which investigates the effect and magnitude of the correction methods to long-term humidity and PW trends.

2.2. GPS

The Global Positioning System (GPS) is a satellite navigation system which provides information about position and time. The fundamental observable of GPS is the signal propagation time from a satellite to a receiver. Due to the atmosphere the signals emitted by the GPS satellites are delayed. This slant path delay, named as “slant total delay” (STD), consists of two parts, “wet delay” and “hydrostatic delay”. The first one depends on water vapour amount along signal’s path. The second one depends on dry gases between receiver and satellite and can be expressed as a function of ground atmospheric pressure. However, for comparison purposes and in calculations, delays are converted to the zenith direction, yielding zenith total delay (ZTD), zenith hydrostatic delay (ZHD) and zenith wet delay (ZWD). This is done by using mapping function, denoted as mf , which depends on the elevation of the received signal, z . In case of total delay mapping, $mf(z)$ is expressed as

$$mf(z) = \frac{STD}{ZTD}. \quad (2.12)$$

In this thesis, a mapping function called Global Mapping Function (GMF) proposed by Boehm *et al.* (2006) is used. It is based on a form proposed by Herring (1992):

$$mf(z) = \frac{1 + \frac{a}{1 + \frac{b}{1 + c}}}{\sin z + \frac{a}{\sin z + \frac{b}{\sin z + c}}}. \quad (2.13)$$

The coefficients a , b and c , depending on the day of the year and the latitude of the site, were determined by the use of monthly mean profiles for pressure,

temperature, and humidity from the European Centre for Medium-Range Weather Forecasts (ECMWF) reanalysis ERA-40 data for the period September 1999 to August 2002. The ZWD is estimated by subtracting the ZHD from the ZTD. The ZHD, depending on the pressure at ground, P_0 , the latitude of the site, λ , and the height of the station, H , is estimated by the equation (Emardson *et al.*, 1998):

$$\text{ZHD} = (2.2767 \pm 0.0015) \frac{P_0}{f(\lambda, H)}, \quad (2.14)$$

where, according to Saastamoinen (1972):

$$f(\lambda, H) = 1 - 2.66 \cdot 10^{-3} \cos(2\lambda) - 2.8 \cdot 10^{-7} H. \quad (2.15)$$

PW is related to the ZWD through a conversion factor, Q :

$$\text{PW} = \frac{\text{ZWD}}{Q}, \quad (2.16)$$

where Q can be found by the following equation (Askne and Nordius, 1987):

$$Q = 10^{-8} \rho_w R_w \left(k'_2 + \frac{k_3}{T_m} \right). \quad (2.17)$$

Here ρ_w is the density of liquid water, 1000 kg/m^3 ; R_w is the specific gas constant for water vapour, $461.5 \text{ J/(kg} \cdot \text{K)}$; $k'_2 = 22.1 \pm 2.2 \text{ K/hPa}$; $k_3 = 373900 \pm 1200 \text{ K}^2/\text{hPa}$; T_m is the mean temperature of the atmosphere in K. In this thesis, T_m is evaluated through the surface air temperature, T_s (Bevis *et al.*, 1992):

$$T_m = 70.2 + 0.72 \cdot T_s. \quad (2.18)$$

It is estimated that the uncertainty of the mean temperature of the atmosphere, $u(T_m)$, is about 2%. The uncertainty of the conversion factor, $u(Q)$, is given as (Ning, 2012):

$$u(Q) = 10^{-8} \rho_w R_w \sqrt{\left(\frac{u(k_3)}{T_m} \right)^2 + u^2(k'_2) + \left(k_3 \frac{u(T_m)}{T_m^2} \right)^2}. \quad (2.19)$$

The total uncertainty of PW is now calculated as follows (Ning, 2012):

$$u(\text{PW}) = \sqrt{\left(\frac{u(\text{ZTD})}{Q}\right)^2 + \left(\frac{2.2767u(P_0)}{f(\lambda, H)Q}\right)^2 + \left(\frac{P_0u(c)}{f(\lambda, H)Q}\right)^2 + \left(\text{PW} \frac{u(Q)}{Q}\right)^2}, \quad (2.20)$$

where P_0 and $u(P_0)$, in hPa, denote the ground pressure and its uncertainty; the $u(\text{ZTD})$ is estimated by standard procedures of the software package. The $u(c) = 0.0015$ represents an uncertainty of the technical parameter c , omitted above for the sake of brevity (Ning, 2012). The uncertainty in PW estimates using GPS has been shown to be slightly above the 1 mm level using data from the Swedish and Finnish networks (Emardson *et al.* 1998; Jakobson *et al.*, 2009).



Figure 2. The GPS station (TOR2) located at Tõravere, Estonia, is a site which belongs to the European Reference Frame Permanent Network (EPN, <http://www.epncb.oma.be/>). The antenna is protected by a hemispheric radome.

2.3. AERONET

Once developed by Fowle (1912) more than a 100 years ago, the spectroscopic technique for PW estimation was not widely used until 1993 when the AERosol RObotic NETwork (AERONET) was started and currently covers with its Cimel photometers more than 400 sites in 50 countries across all seven continents. The retrieval of PW is based on direct Sun radiation measurements at 940 nm using the Bouguer-Lambert-Beer law. According to this law, the digital voltage of the instrument $V(940 \text{ nm})$ is given by (Halthore *et al.*, 1997; Schmid *et al.*, 2001):

$$V(940 \text{ nm}) = V_0(940 \text{ nm})d^{-2} \exp(-m\delta_{\text{atm}}(940 \text{ nm}))T_w(940 \text{ nm}), \quad (2.21)$$

where $V_0(940 \text{ nm})$ is a hypothetical voltage that the instrument would measure at the top of the atmosphere (obtained through the calibration procedure); d is the relative Earth-Sun distance at the time of observation; m is optical air mass; $\delta_{\text{atm}}(940 \text{ nm})$ is the total atmospheric optical depth (excluding absorption by water vapour but including Rayleigh scattering, absorption and scattering due to aerosol as well as gas absorption mainly due to O_3 and NO_2); $T_w(940 \text{ nm})$ is the transmittance due to water vapour. The latter is given by (Halthore *et al.*, 1997; Schmid *et al.*, 2001; Smirnov *et al.*, 2004):

$$T_w(940 \text{ nm}) = \exp(-a(m_w \text{PW})^b), \quad (2.22)$$

where m_w is the optical water vapour air mass and coefficients a and b are filter-dependant constants. After combining Equations (2.21) and (2.22), the following equation is formed (Pérez-Ramírez *et al.*, 2014):

$$\text{PW} = \sqrt[b]{\frac{\ln V_0(940 \text{ nm}) - \ln V(940 \text{ nm}) - \delta_{\text{atm}}(940 \text{ nm})m}{am_w^b}}, \quad (2.23)$$

Although, this method provides relatively good temporal resolution of PW with an uncertainty of 10% (Holben *et al.*, 2001), it has some significant drawbacks. First, measurements made by photometers require a clear solar disc, thereby offering only daytime data biased towards cloud-free conditions. Secondly, due to low elevation angles of the Sun, the method is less available during winter at high latitudes. In the AERONET network, this period of inactivity is usually used for service and laboratory calibration of photometers. One of its Sun photometers, Cimel 318A, is used at Tõravere (Estonia) since June 2002. The AERONET data are freely available at their website (AERONET, 2015).



Figure 3. An AERONET sunphotometer Cimel 318A working at a weather station located in Tõravere, Estonia.

2.4. Regional and global models

To make physical sense of observational data, estimate the state of the atmosphere and investigate possible changes, a model is needed. These models provide a basis for forecasting weather and future climate. The database of operational weather forecast High Resolution Limited Area Model (HIRLAM) was used in comparisons carried out at Tõravere, Estonia (see Chapter 5). The model output covers the area of Europe from 45 °N northward and consists of two parts. First, it is updated four times daily, at 00, 06, 12 and 18 UTC, by reports from meteorological networks, and secondly, it produces forecasts for 03, 09, 15, 21 UTC. The HIRLAM version 7.1.4, used to retrieve PW values in this thesis, has a 0.1-degree horizontal and 60-layer vertical resolution. Estimation of uncertainty in PW retrievals by numerical weather prediction (NWP) models (e.g. HIRLAM) is complicated. Apparently, the uncertainty depends, besides the density of ground-based meteorological network, also on the closeness of upper-air sounding stations and daily frequency of ascents.

While operational NWP models are constantly improved, reanalyses are based on a consistent method to reprocess observational data, producing a valuable dataset for weather and climate research. Although, there are

reanalyses that extend over hundred years, most of them cover the period since 1979, which marked the beginning of the satellite era.

In this thesis, the datasets from two of the most recent reanalyses have been used for investigation of PW's diurnal cycle over the Baltic Region in summer (see Chapter 4):

- first, National Centre of Environmental Predictions – Climate Forecast System Reanalysis (NCEP-CFSR, USA), being a global reanalysis, has a 0.5-degree horizontal, 64-layer vertical and 6-hour temporal resolution (Saha *et al.*, 2010);
- secondly, regional reanalysis BaltAn65+, obtaining the boundary fields from the ECMWF ERA-40 reanalyses, is based on HIRLAM version 7.1.4 and has a 0.1-degree horizontal, 60-layer vertical and 6-hour temporal resolution (Luhamaa *et al.*, 2010).

In addition to NCEP-CFSR, four reanalyses were tested against independent tetheredsonde data in the Arctic (see Section 5.2):

- first, a global reanalysis ERA-Interim, developed by the ECMWF and based on the data assimilation system rooted in 2006, has a spatial resolution of 0.75-degree horizontal, 60-layer vertical and 6-hour temporal resolution (Dee *et al.*, 2011);
- secondly, the Japan Meteorological Agency (JMA) has developed a global reanalysis called JMA Climate Data Assimilation System (JCDAS), covering the period from January 2005 to present. Being a continuation of the JRA-25 (Onogi *et al.*, 2007), it has 1.25-degree horizontal, 40-layer vertical and 6-hour temporal resolution;
- thirdly, NCEP together with U.S. Department of Energy has produced a reanalysis NCEP-DOE, which has 2.5-degree horizontal, 28-layer vertical and 6-hour temporal resolution (Kanamitsu *et al.*, 2002);
- fourthly, NASA Modern Era Retrospective-Analysis for Research and Applications (MERRA), with 1.25-degree horizontal, 42-layer vertical and 3-hour temporal resolution, was used (Cullather and Bosilovich, 2011).

Assessment of the uncertainties in reanalyses output, together with the biases in models and observations, remains the most difficult challenge for the reanalysis and data assimilation community (Bosilovich *et al.*, 2013).

2.5. Data processing

To estimate variations and trends in atmospheric humidity and temperature since 1980s (Chapter 3), the data from four radiosonde stations were involved (Fig. 4):

- Harku (59.38 °N, 24.58 °E), 1998–2012, 4928 soundings;
- Jokioinen (60.81 °N, 23.50 °E), 1982–2012, 10 934 soundings;

- Jyväskylä (62.40 °N, 25.68 °E), 1982–2012, 10 946 soundings;
- Sodankylä (67.36 °N, 26.65 °E), 1982–2012, 10 974 soundings.

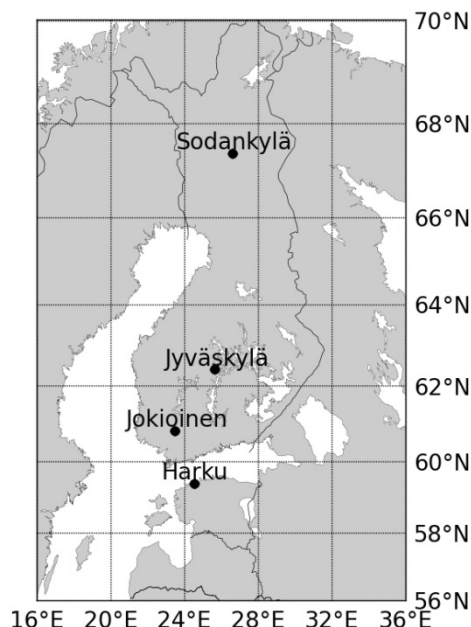


Figure 4. Map of the four radiosonde stations used in long-term temperature and humidity analysis.

Low-resolution humidity and temperature profiles (consisting of about 30–60 levels) for stations in Finland were retrieved from a freely accessible web site of the University of Wyoming (<http://weather.uwyo.edu/upperair/sounding.html>). For Harku (Estonia), high-resolution profiles (measurements at every 2–10 s) from the Estonian Environment Agency were used.

Only measurements at 00 UTC were used, except for Jyväskylä, where due to the shift of the launching time, since 1997 soundings at 06 UTC were used instead. Radiosonde profiles were vertically linearly interpolated with the step of 500 m from ground. Monthly means at all levels were calculated by averaging at least 6 measurements. By this condition, the highest level available for trend calculations was determined. Linear regression analysis used in this thesis for the detection of trends requires a normal distribution of data. This requirement was satisfied when investigating annual and monthly values of temperature and specific humidity, being a suitable method for trend calculations. All trends were considered to be statistically significant at 95% confidence level.

The correction for improving the accuracy of RH at low temperatures by restoring more detailed original humidity profiles using the time-lag correction has the restriction that only time resolved RS80-A data can be used. In this

work, high-resolution data from one station, Harku, were analysed. Despite the fact that RS80-A was in use from 1993 to 1998, the digitalized high-resolution data were available since 1998. The data collected at Harku in 1998 were used for estimating the impact of different corrections proposed for eliminating the main errors in RS80-A RH measurements.

When homogenizing radiosonde data, one must remember that the bias corrections are mean corrections based on comparisons with the cryogenic frost point hygrometer (Vömel *et al.*, 2007b) and some laboratory work. This means that on a larger data set, the mean bias should be reduced to zero. However, there is a scatter in the behavior of individual sondes, some needing more others needing less correction. Therefore, it is very well possible, that some sondes are overcorrected showing RH values above 100%. These are real measurements with an uncertainty that is large enough to include 100% RH. Although the value itself is physically not very likely, one should treat this value like any other number below 100%, which may have the same level of uncertainty. In operational systems readings above 100% and below 0% are cut off. This kind of constraining was not applied, since it will create biases over a larger set of soundings.

To investigate diurnal cycle of PW (Chapter 4), data for the overlapping period 1979–2005 from two reanalyses, NCEP-CFSR and BaltAn65+, were analysed. The BaltAn65+ data from 1965–1978 were omitted in order to keep the periods closer and to avoid systematic errors that ERA-40 had before the satellite era (Jakobson and Vihma, 2010). NCEP-CFSR data from 2006–2010 were left out, so that only data from the same period would be compared. The study area is 53–68 °N, 12–32 °E. All calculations correspond to the UTC time.

To intercompare different PW estimation techniques available in Estonia, two observation campaigns at Tõravere (58.26 °N, 26.47 °E, 70 m) were performed (Sections 5.1.1 and 5.1.2). During the considerably longer campaign from 22 June to 6 November 2008, the PW retrievals by AERONET, GPS and HIRLAM were available. The GPS database included 3264 hourly averaged PW values on 139 days. The HIRLAM database, including its both parts (reports from the meteorological networks and predictions, respectively), enables to estimate humidity profiles and therefore, PW values, with a 3-h step. HIRLAM (Version 7.1.2) produced 1105 PW values for 138 days. Retrievals from GPS and HIRLAM were linearly interpolated to the times when the AERONET-measured PW values were available.

During the shorter campaign from 9 to 12 August 2010, data obtained by means of four methods – radiosonde, AERONET, GPS, and HIRLAM – were available. 17 sondes were launched by the Estonian Defence Forces with the time interval of three hours. For intercomparison with other methods, hourly means for AERONET and GPS measurements were calculated.

Besides finding the largest discrepancies between single measurements, in order to quantify and evaluate the rate of differences between pairs of methods, six simple statistical tests were employed. The mean bias difference (MBD and

MBD%) reveals the average systematic deviation of PW by Method2 as y compared to Method1 as x (or reference in this comparison):

$$\text{MBD} = \frac{1}{N} \sum_{i=1}^N (y_i - x_i) , \quad (2.24)$$

$$\text{MBD}\% = \frac{1}{N} \sum_{i=1}^N \frac{y_i - x_i}{x_i} 100\% . \quad (2.25)$$

Here N denotes the number of concurrent measurements during the campaign. Scatter between two methods was quantified by the root-mean-square difference (RMSD and RMSD%):

$$\text{RMSD} = \left\{ \frac{1}{N} \sum_{i=1}^N (y_i - x_i)^2 \right\}^{1/2} , \quad (2.26)$$

$$\text{RMSD}\% = \left\{ \frac{1}{N} \sum_{i=1}^N \frac{(y_i - x_i)^2}{x_i^2} \right\}^{1/2} 100\% . \quad (2.27)$$

The fifth statistical test was calculation of a slope, a , for least squares linear fits, $y = ax$. In order to quantify a rate of consistency of two simultaneous estimations of PW, a concept proposed by Immler *et al.* (2010) was used. A rate of consistency of measurements was checked according to fulfilment of inequality:

$$|x_i - y_i| < k \cdot \sqrt{u_x^2 + u_y^2} , \quad (2.28)$$

where two independent simultaneous measurements of PW are denoted with x_i and y_i and their standard uncertainties u_x and u_y , respectively; coverage factor, $k = 1, 2, 3$ is a numerical multiplier to obtain an expanded uncertainty (GUM, 1995). Terminology for checking the consistency of x_i and y_i is given in Table 1.

Table 1. Terminology for checking a pair of independent measurements for consistency

Fulfilment of condition, equation (2.28)	Evaluation
$k = 1$	Strong consistency
$k = 2$	Moderate consistency
$k = 3$	Weak consistency

If condition by Equation (2.28) is not valid even for $k = 3$, the pair of measurements is considered as inconsistent.

Regarding the validation of reanalyses over the Arctic, a total of 95 tethersonde soundings during 39 sounding days from 25 April to 31 August 2007 were made (Section 5.2). The Vaisala DigiCORA Tethersonde System was used to measure the vertical profiles of the air temperature, RH, wind speed, and wind direction up to the height of 2 km. The measurement system consisted of three tethersondes at approximately 15 m intervals in the vertical, attached to a tethered balloon. The balloon was ascended and descended with a constant speed of approximately 1 m s^{-1} . The tethersonde system was only operated in non-precipitating conditions (except of very light snow fall) with wind speeds less than 15 m s^{-1} , and it was not ascended into thick clouds. The data of temperature and humidity were averaged over the three tethersondes using a 20 m averaging interval. The average top height of the soundings was 1240 m. In this study, 29 profiles up to 890 m were used; to avoid giving excessive weight to data from days with a high sounding activity, only the profile that reached the highest altitude from each day was selected. The profiles selected for this study were measured between 09 and 18 UTC. The closest reanalysis output time was always selected for validation. The value of RMSE was calculated similarly to the Equation (2.26).

3. LONG-TERM VARIATIONS AND TRENDS

Global climate variability and warming has been widely debated topic for many years all over the world. Comprehensive studies have been made also for the Baltic Region, for example by Jaagus (2006) and Tuomenvirta (2004). Research by Jaagus involved surface air temperature (T_s) trend analyses during the years 1951–2000 in Estonia. Statistically significant increasing trends in T_s were detected in January, February, March, April and May (annual trend 0.2–0.35 °C (10 yr)⁻¹). Similar study for Finland was conducted by Tuomenvirta, who reported annual T_s trend 0.08 °C (10 yr)⁻¹ for the 20th century. For the period 1976–2000, the trend was as much as 0.81 °C (10 yr)⁻¹.

These warming trends at surface refer to an exponential increase of the PW (Gaffen *et al.*, 1992). On contrary to T_s , tropospheric temperature and humidity trends are investigated considerably less. Regarding the climate warming, it has been shown that the middle and upper troposphere are responsible for almost all of the infrared water vapour feedback, leaving only 10% to be contributed by the layer below 2 km, showing the necessity to evaluate tropospheric humidity at higher altitudes with high accuracy (Spencer and Braswell, 1997; Held and Soden, 2000). In addition, the global surface climate has shown to be significantly driven by the water vapour in the stratosphere, which has a cooling effect on the stratosphere but warming effect on the troposphere (Solomon *et al.*, 2010). At the same time, early radiosonde sensors have been known to suffer from significant measurement biases in humidity, particularly for the upper troposphere, and changes in instrumentation with time have resulted in discontinuities in the data record. Consequently, most of the analyses of radiosonde humidity have focused on trends for altitudes below 500 hPa (5.5 km) and are restricted to those stations and periods for which stable instrumentation is available (Trenberth *et al.*, 2007). In this section, the variations and trends in PW, SH and temperature over Estonia (Harku) as well as Finland (Sodankylä, Jokioinen and Jyväskylä) by means of Vaisala RS80-A, RS90 and RS92 radiosondes are discussed. In addition, the impact of different corrections on radiosonde humidity records is evaluated.

3.1. Impact of the radiosonde corrections on humidity

In order to assess the necessity of applying different corrections to retrieve homogeneous PW dataset, the impact of time-lag (TL) and temperature-dependence (TD) corrections on RS80-A humidity was investigated. The results were retrieved for the year 1998 at Harku, when RS80-A was still in use and its high-resolution measurements were available, thereby offering the opportunity to apply also the TL correction proposed by Miloshevich *et al.* (2004).

Fig. 5 indicates that by using TD correction developed by Miloshevich *et al.* (2001), TD-M, the yearly average RH was increased with the maximum of 13%

just above the tropopause. At the same time, TD-M had almost no impact on humidity at temperatures higher than -15°C (below 4 km). Above this height, in terms of SH, TD-M had an increasing effect up to 12 km. However, since a major part of water vapour lies in the lowermost layers, TD-M increased PW only by 0.5%. The multiplicative correction factors in single RS80-A RH profiles at the lowest temperatures reached up to 2.8.

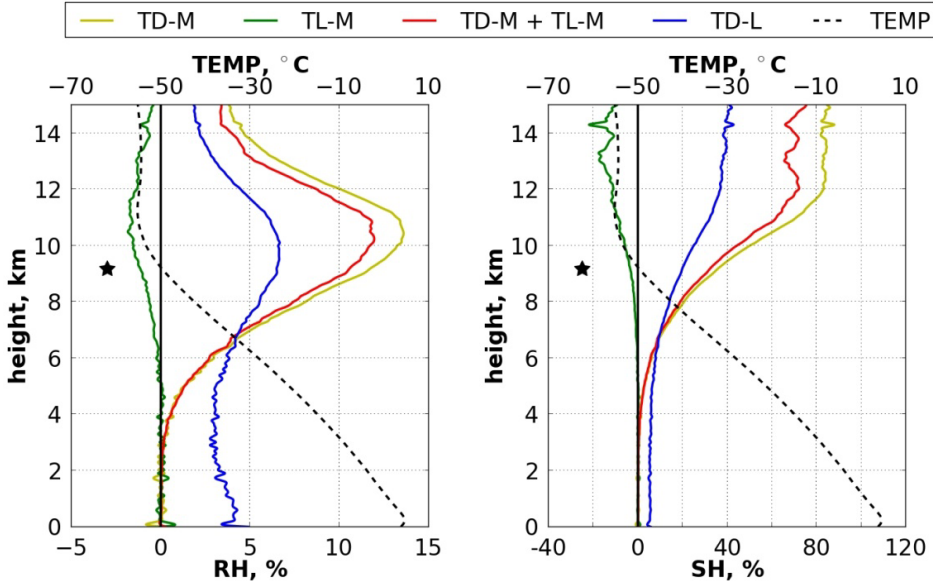


Figure 5. Impact (in percents) of different corrections on annual relative humidity (RH) and specific humidity (SH) profiles at Harku, based on data retrieved in 1998. Corrections are drawn with continuous lines as follows: a) yellow: temperature-dependence correction, Miloshevitch *et al.* (2001); b) blue: temperature-dependence correction, Leiterer *et al.* (2005); c) green: time-lag correction, Miloshevitch *et al.* (2004); d) red: sum of the two corrections by Miloshevitch *et al.* Temperature profile is drawn by a dashed black line and the average altitude of the tropopause (9 137 m) is shown by a black star.

The correction eliminating the TL error (Miloshevitch *et al.* 2004), TL-M, had a significantly smaller effect on humidity than TD-M. The yearly average RH which was corrected for TL error only, was decreased with the maximum of 2% at the lowest temperatures, having almost no effect on annual PW value. This was an expected finding, while TL error only leads to systematic biases in climatological records at altitudes, where the sign of the vertical RH-gradient is always decreasing, i.e. above the tropopause. Nevertheless, TL-M correction factors in single RS80-A RH profiles at low temperatures and rapidly changing RH values reached up to 8.5. Therefore, in such exceptional cases, TL error may be a dominant error in single RH profiles.

On the other hand, TD correction proposed by Leiterer *et al.* (2005), TD-L, has a more pronounced effect compared to TD-M below 6.5 km (above -30°C). This is in a good agreement with the study by Suortti *et al.* (2008) on a shorter period. Clearly, the magnitude of the TD-L depends on the RH profile. The study carried out by Finnish colleagues pays attention mainly to conditions where thick clouds are present, correcting RH values more than seen in Fig. 5. Yearly RH values in the upper troposphere at Harku are much lower due to the fact that the yearly average condition is “less cloudy”. Fig. 5 revealed that the effect of TD-L to the yearly SH profile is increasing with height, rising tropospheric SH values by 3–20% and causing an average increase in PW of 4%.

Based on the fact that the TD-L has proved to have advantages over the TD-M in the lower and mid troposphere, where it has major impact on PW, and the outcome of this work derived from data collected during considerably longer period is comparable to the results by Suortti *et al.* (2008), long-term trends corrected only using TD-L were investigated.

3.2. Yearly trends

Annual anomalies of SH during 1982–2012 at three Finnish radiosonde stations (Fig. 6) and during 1998–2012 at Harku, Estonia (Fig. 7), were analysed. Studying data retrieved at Finnish stations, exceptionally high positive anomalies (up to 35% from the average SH value) in mid troposphere in the beginning of the radiosonde record around 1982–1984 were revealed. These anomalies had a diminishing effect on SH trends at higher altitudes. At the same time, large positive anomalies in temperature during 1982–1984 were not found. It is followed by the coldest – although, not the driest – period around 1985–1987. For all stations in Finland, annual anomalies of SH near to the ground appear to be the most negative during 1993–1994 (also resulting in the lowest annual PW values in Fig. 8). The late 1990s are relatively warm and moist, the same tendency is evolving in recent years.

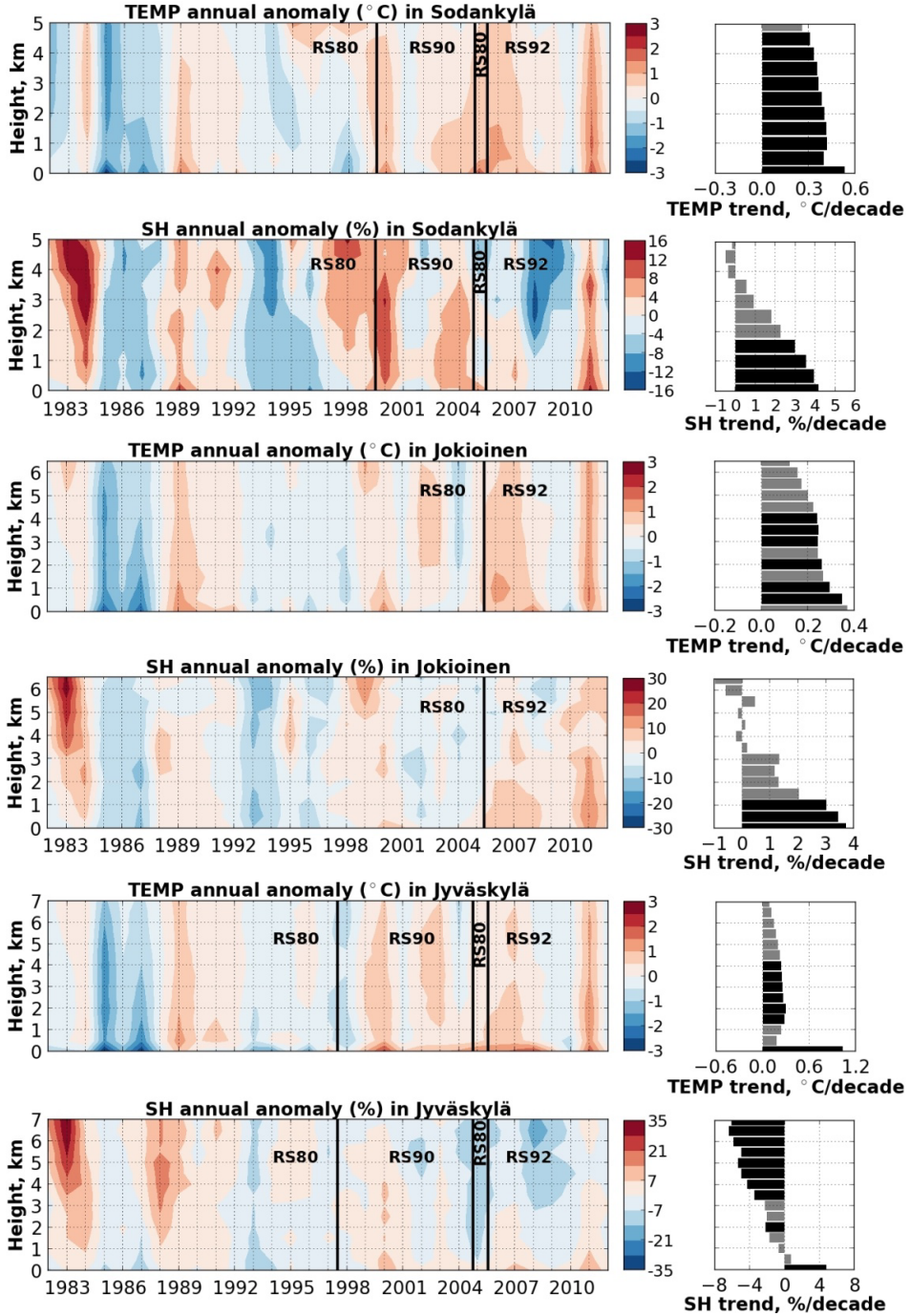


Figure 6. Annual anomalies of temperature ($^{\circ}\text{C}$) and specific humidity (SH, %) as well as their trends (plots on right) at stations in Finland. Statistically significant trends at the 95% confidence level are marked with black horizontal bars in right panels, while statistically insignificant ones are marked with grey bars. Anomalies are calculated for each level from the mean of the whole period, 1982–2012. Sonde transitions from one type to another are marked with black vertical lines.

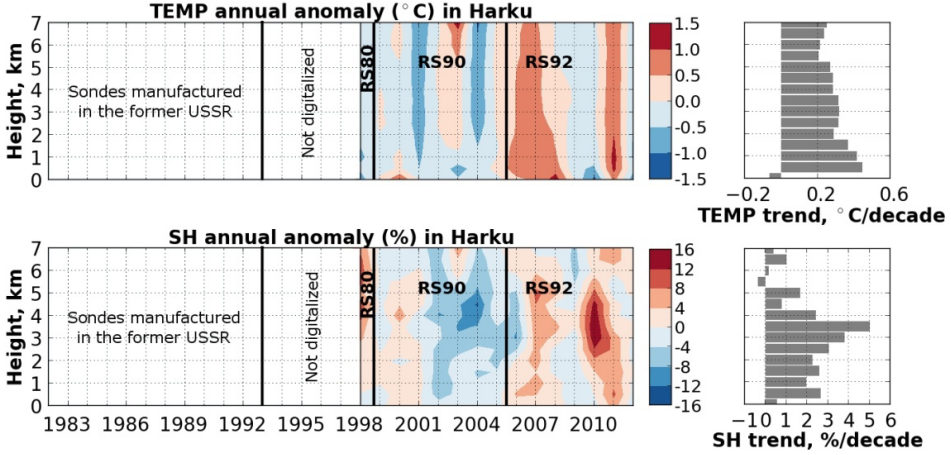


Figure 7. Same as Fig. 6, but explaining the variability at Harku, Estonia. Only the humidity data from the year 1998, when RS80-A was used, were corrected. Contrary to the stations in Finland, no statistically significant trends were found (all bars marked with grey).

As seen from Fig. 6, trends in SH near ground are positive, while at higher levels they diminish or are mainly negative. According to the August-Roche-Magnus approximation (often called just Magnus approximation) for Clausius–Clapeyron equation, the water holding capacity of the atmosphere (here saturation water vapour pressure, e_s) increases exponentially with temperature (August, 1828; Magnus, 1844; Lawrence, 2005):

$$e_s = C_1 \exp\left(\frac{A_1 t}{B_1 + t}\right), \quad (3.1)$$

where t is temperature in degrees Celsius. Alduchov and Eskridge (1996) recommended the following values for the coefficients $A_1 = 17.625$, $B_1 = 243.04$ °C and $C_1 = 6.1094$ hPa. By using these values, the water holding capacity of the atmosphere increases by about 7% per degree Celsius increase in temperature, assuming a constant RH. In other words, PW should increase by 7% if there is a warming by 1 °C apparent throughout the troposphere and RH does not change. Near ground, SH trend follows the magnitude as described by this equation because negative trends in RH are relatively small $<1\%$ $(10 \text{ yr})^{-1}$ (not shown). However, at higher altitudes, RH has statistically significant trends up to -4% $(10 \text{ yr})^{-1}$, explaining the different rate per degree Celsius than 7% as assumed by the Equation (3.1). In some cases (e.g. at Jyväskylä above 2 km level), it is resulted even in opposite trend signs of temperature and SH.

Obviously, when the values at the beginning or the end of the dataset are considerably increased or decreased, it also causes a change in the value of the

trend. By increasing SH values at all altitudes throughout the troposphere, TD-L changed the values of the trends at three Finnish stations towards negative values by 2–3% (10 yr)⁻¹. Applying TD-L raised annual PW before 2001 by about 4–5%. Since 2001, the mean dry bias in TD-L is reduced, resulting in significantly smaller rise in PW.

Annual anomalies in PW in Fig. 8 reach up to 10%. Due to the fact that trends in SH at different altitudes were relatively small or even below the level of the significance, trends in annual PW were not found at any of the stations studied. Moreover, probably because the data record is relatively short, none of the statistically significant trends in annual temperature, RH and SH were identified at Harku.

Annual anomalies in temperature are the highest at ground, reaching up to 3 °C. In Finland, from 1982 to 2012, there has been a positive annual T_s trend at two stations, Jyväskylä and Sodankylä, 1.0 °C (10 yr)⁻¹ and 0.5 °C (10 yr)⁻¹, respectively. This agrees well with the similar study for Finland conducted by Tuomenvirta (2004). Below 2 km, all statistically significant temperature trends at the 95% confidence level have found to be positive, ranging from 0.3–1.0 °C (10 yr)⁻¹.

Using radiosonde data from 50 stations around the world for 1973–1990, Gaffen *et al.* (1992) showed that the relationship between PW and surface air temperature, T_s , is well described by a linear equation:

$$\ln PW = a \cdot T_s + b, \quad (3.2)$$

coefficients a and b depending on the T_s range considered and the coefficient of determination between their monthly values, $R^2 = 0.88$. The latter is even higher for stations poleward of the 20° latitude. In addition, the correlation between these two characteristics increases when comparing yearly averages, since mean values over a longer period give rise to uniformity in the vertical humidity profile. By taking into account only the yearly surface air temperature at stations in Finland and using the Equation (3.2), PW increases by 5–6% °C⁻¹. The coefficient of determination, R^2 , ranges from 0.75 to 0.80 for individual measurements and from 0.92 to 0.96 for monthly values.

Analyse involving nearly 11 000 soundings from each of the stations in Finland confirmed the finding reported by Okulov *et al.* (2002), that PW more strongly is related to the surface water vapour pressure, e_0 , than to the surface air temperature. A linear form:

$$PW = a \cdot e_0 + b, \quad (3.3)$$

was also used in this thesis. Regarding the relationship between e_0 and PW, the coefficient of determination, R^2 , ranges from 0.82 to 0.85 for individual measurements and from 0.95 to 0.98 for monthly values. While the relationship

between those characteristics is linear, the change in PW per hPa increase in e_0 is in absolute units and varies from 2 to 3 mm hPa⁻¹.

To conclude, based on the homogenized dataset, trends in SH and temperature in all of the stations are relatively small, if statistically significant at all. Investigating PW long-term variability and trends, datasets retrieved by RS80-A and newer Vaisala radiosondes should not be united without homogenizing, because a correction method by Leiterer *et al.* (2005) increases the yearly PW significantly.

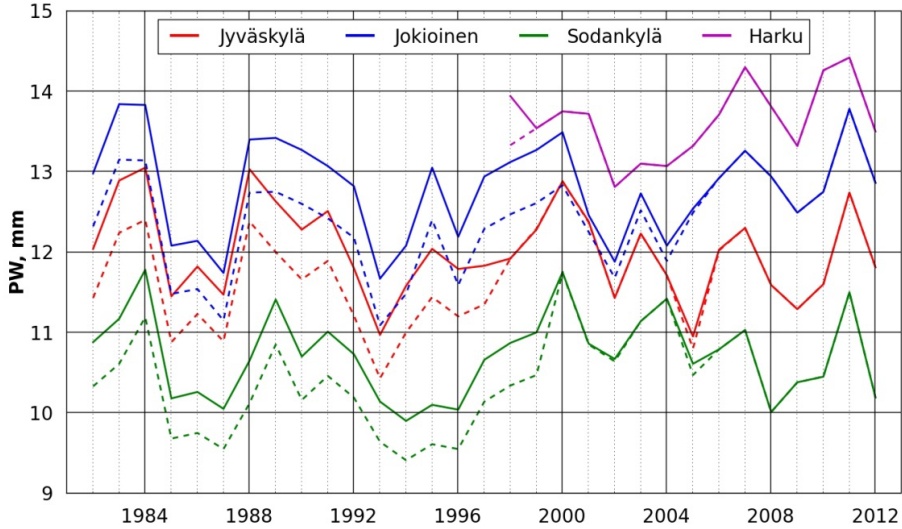


Figure 8. Annual PW values at Jyväskylä, Jokioinen, Sodankylä and Harku. PW values calculated from uncorrected profiles of the RS80-A are marked with dashed line, corrected PW values with continuous line. Inclusion of the temperature-dependence correction by Leiterer *et al.* (2005) has a major impact on annual PW, rising its value by about 4%. Trend in annual PW was not found at any of the stations studied.

3.3. Monthly trends

Similarly to the yearly trends, monthly trends during 1982–2012 at three Finnish radiosonde stations and during 1998–2012 at Harku (Estonia) were analysed (Fig. 9). Monthly trends in SH differ from station to station and are inhomogeneous by means of altitude and month. Most positive SH trends up to 10% (10 yr)⁻¹ at stations in Finland are detected during August, September and October. Trends in SH above 3 km are mainly negative, showing values up to -12.6% (10 yr)⁻¹.

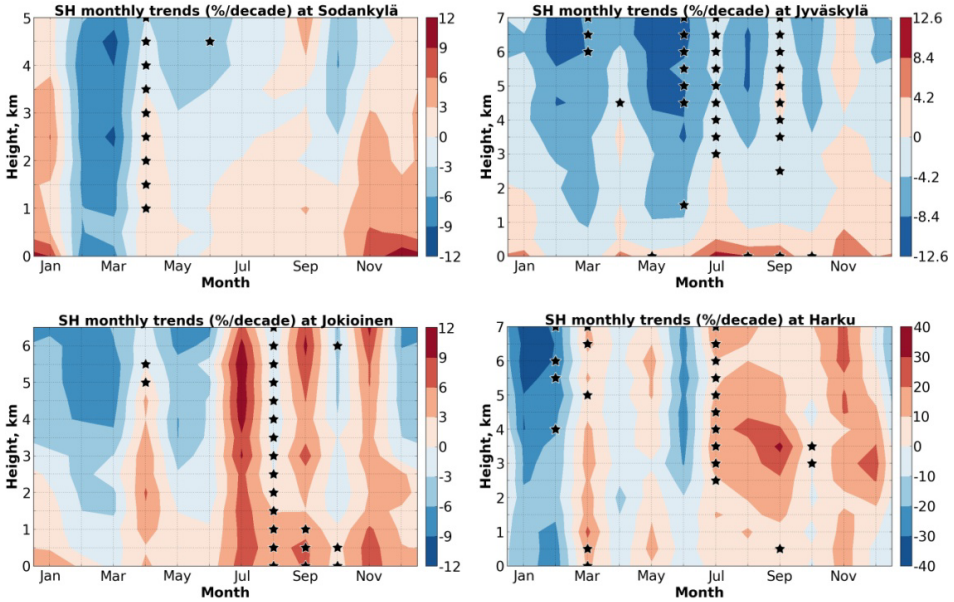


Figure 9. Trends in specific humidity (% per 10 yr) at Sodankylä, Jyväskylä, Jokioinen and Harku. Statistically significant trends at the 95% confidence level are marked with black stars. These trends are based on the data collected during 1982–2012 at stations in Finland and during 1998–2012 at Harku. Precipitable water, most affected by the magnitude of changes in specific humidity at lower tropospheric levels, has a negative trend at Sodankylä in March, $-0.5 \text{ mm (10 yr)}^{-1}$, while positive trends have appeared at Jokioinen in July, $1.5 \text{ mm (10 yr)}^{-1}$, and at Harku in September, $2.2 \text{ mm (10 yr)}^{-1}$.

If SH trends were investigated in units g kg^{-1} , these would have been largest near ground, because the profile of SH decreases exponentially with height. Its monthly value at ground in summer ranges from 7 to 11 g kg^{-1} , while its value at 6 km level ranges from 0.7 to 1.3 g kg^{-1} , depending on the latitude of the site. In winter, its values at those levels are $1\text{--}3 \text{ g kg}^{-1}$ and $0.1\text{--}0.6 \text{ g kg}^{-1}$, respectively. Due to the spatial distribution of water vapour, trends in monthly PW are not necessarily determined by statistically significant trends in SH profiles, but depend mainly on the magnitude of the changes in SH at lower tropospheric levels. For example, PW has a negative trend at Sodankylä in March, $-0.5 \text{ mm (10 yr)}^{-1}$, when strong negative trends, although insignificant ones, in SH are apparent. This trend in PW, in turn, is significantly related to the decrease in North Atlantic Oscillation (NAO) index during this month. The latter shows fluctuations in the differences of sea-level pressure between a permanent low-pressure system over Iceland and permanent high-pressure system over Azores. Its monthly values have been drawn from the website of the National Oceanic and Atmospheric Administration (NOAA, 2014). Positive PW trends have appeared at Jokioinen in July, $1.5 \text{ mm (10 yr)}^{-1}$, and at Harku in September, $2.2 \text{ mm (10 yr)}^{-1}$, both not explained by the changes in NAO index.

On the whole, while neither PW nor NAO index has a statistically significant trend at the 95% confidence level during winter (December, January, February), these two components are loosely but significantly related during winter period at all four stations. The correlation coefficient, r , between winter averages of PW and NAO index ranges from 0.47 to 0.55.

Correlation was also investigated between monthly SH and NAO index at different altitudes (Fig. 10). Again, most of the statistically significant correlation coefficients were detected during the cold period. Correlation is the strongest below 2 km level, where coefficients reach up to 0.8 in January, February and March. Moreover, monthly SH profile depends clearly on NAO index even in April and November. However, the relationship in those months is weaker than during January, February and March. Generally, the rate of the correlation during winter decreases by height. Correlation coefficients between monthly SH and NAO index in July, August and September are mainly negative, but only some of them have found to be statistically significant. While radiosonde-derived SH is calculated from RH and temperature measurements, relationships between monthly RH and NAO index as well as temperature and NAO index were investigated. It was revealed that temperature and NAO index correlate more strongly than RH and NAO index. Therefore, it can be said that NAO affects atmospheric humidity content at the stations studied mainly through an increase and decrease in temperature.

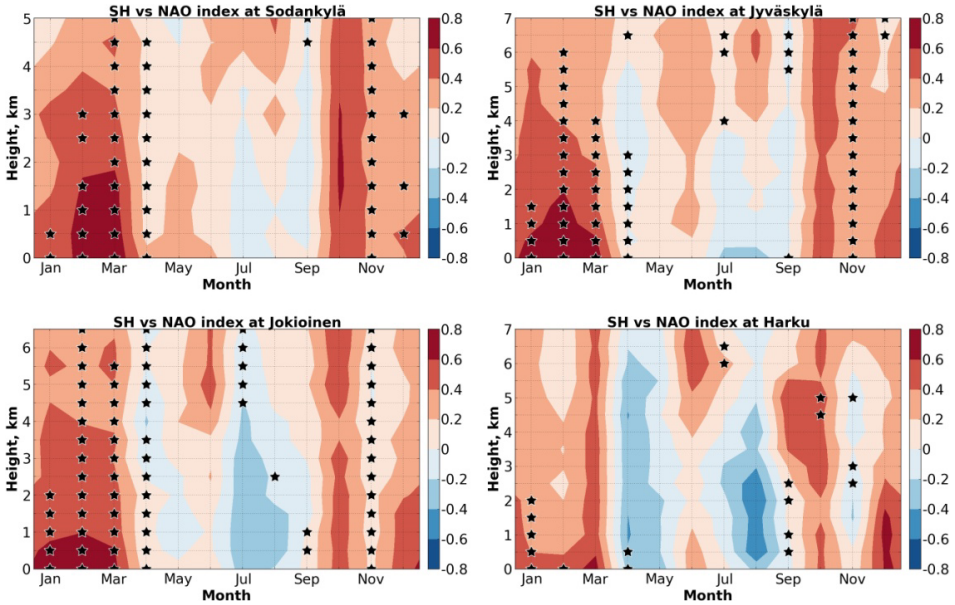


Figure 10. Correlation coefficients between specific humidity (SH) and North Atlantic Oscillation (NAO) index at Sodankylä, Jyväskylä, Jokioinen and Harku. Statistically significant relationships at the 95% confidence level are marked with black stars. Correlation is the strongest during January, February and March below 2 km level, where correlation coefficients reach up to 0.8.

The results presented here are in a good agreement with finding by Jaagus (2006). According to the study based on investigation of data from the second half of the 20th century, the strongest relationship between NAO index and temperature as well as precipitation above Estonia is specific for the winter period. Although, wind profiles were not investigated, the study made by Keevallik (2003) revealed that the NAO index and the zonal component of the wind over Estonia are strongly correlated. This means, an increase in PW and SH (especially below 2 km) during winter is partly caused by the stronger winds from SW and WSW, carrying relatively warmer and somewhat humid air from the Atlantic to Estonia and Finland, causing mild weather. The opposite is true for a decrease. A decrease in PW and SH during winter refer to the relatively weaker winds from SW and WSW, resulting in a cold winter.

4. DIURNAL CYCLE

Similarly to the seasonal variability of PW, the diurnal variability of PW depends on geographical location and is affected by several factors: atmospheric large-scale motion, evaporation and condensation, vertical mixing as well as local winds driven by the sea breeze circulation in coastal areas (Dai *et al.*, 1999a, 1999b, 2002; Ortiz de Galisteo *et al.*, 2011). All these factors mentioned are closely related to each other through changes in solar radiation which drives the humidity cycle via the temperature cycle. So far, only few studies have been dedicated to the diurnal cycle of humidity in the Baltic Region. All of them have investigated data over land, some even showing opposite findings about the timing of its maximum and minimum values (Bouma and Stoew, 2001; Bouma, 2002; Jakobson *et al.*, 2009; Okulov and Ohvri, 2010). Neglecting the importance of the atmospheric large-scale motion to the diurnal cycle of humidity by smoothing out its variability using extended datasets from global reanalyses for 1979–2005, the study revealed that the diurnal cycle at summer depends on whether the area of investigation is located above the Baltic Sea and larger lakes, or above the land.

4.1. Diurnal cycle depending on the underlying surface and sea/land breeze

According to the both reanalyses, BaltAn65+ as well as NCEP-CFSR, the sign and magnitude of the diurnal changes are similar for the same underlying surface (Fig. 11). In summer, the cycle is influenced by the sea and land breeze circulation. The former develops due to the fact, that the solar radiation heats land more quickly than water because their different heat capacity. Then, relatively colder air from the sea is transported to areas above the land where it warms, ascends and returns to the sea as a downward flow, resulting in an increase of PW above the land and decrease above the water. The latter develops at night when land has already cooled down and the sea is relatively warmer. Then, the cycle is reversed. According to the Fig. 11, a typical PW diurnal cycle over the Baltic Region at summer is described as follows.

- At night, from 00 to 06 UTC, a decrease up to 5% in atmospheric humidity above the land is notable and PW reaches its daily minimum. This is caused by the minimum in temperature profile and downward transport of water vapour, resulting in fog and dew, that allows water vapour to condensate on ground and vegetation. While below 950 hPa (500 m) SH is increasing, above that level a decrease is seen. On the other hand, the sea is left without significant changes.
- From 06 to 12 UTC, an opposite effect above the land is obvious, when PW is increasing especially at the eastern part of the Baltic Region. The temperature has increased in the whole profile. The change in SH does not

reflect the change in temperature in detail, showing a decrease below 950 hPa and an increase above that level. This is a result of intensive upward convective transport which carries water vapour to higher altitudes more quickly than it is added through evaporation. At the same time, PW decreases due to the downward flow all over the Baltic Sea by the same magnitude as the decrease above the land was apparent 6 hours ago.

- From 12 to 18 UTC, the changes above the water and land are still in the same direction as 6 hours ago, however, their magnitude is smaller except above the land in the western part of the Baltic Region. An increase in SH above the land can be described by the weakening of the turbulent mixing, allowing water vapour to stay near to the ground (at 1000 hPa) as was seen from the SH profile.
- From 18 to 00 UTC, the signs of the changes are reversed. Above the ground the decrease in temperature below 900 hPa (1 km) has also caused a decrease in humidity. In contrast, due to the land breeze, humidity above the water has now reached a peak.

Investigation of winds over the Baltic Region suggested that land breeze at 00 UTC and sea breeze at 12 UTC affect the diurnal cycle of PW all over the Baltic Sea and larger lakes (Ladoga and Vänern) by transporting humidity below the 900 hPa (1 km) level. The sea breeze has the ability about the same magnitude to penetrate inland as the land breeze to spread out to sea, reaching more than 100 km from the coast.

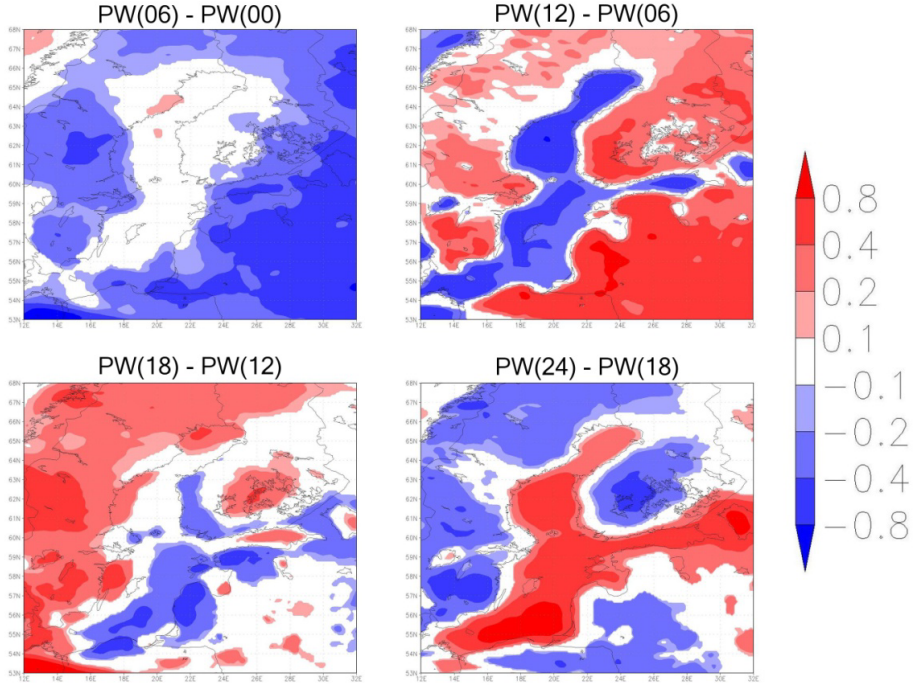


Figure 11. Summer (JJA) differences in precipitable water, PW [mm], as calculated from BaltAn65+ for 1979–2005 between different UTC hours. Humidity content above the water reaches a peak and decreases to the minimum at 00 UTC and 18 UTC, respectively. Above the land the peak is reached at 18 UTC and the minimum is detected at 06 UTC.

4.2. Layers responsible for diurnal cycle

To estimate the influence of different atmospheric layers on PW diurnal variation, the PW difference between 18 and 06 UTC ($dPW = PW_{18 \text{ UTC}} - PW_{06 \text{ UTC}}$) was calculated, as this time interval usually gives the largest differences in PW. After that, the contributions to dPW from vertical intervals 900–1000 hPa, 800–900 hPa and 800–1000 hPa were calculated (Fig. 12). Humidity variations in the lowest interval from 900 to 1000 hPa affect PW diurnal variability more above the water than the land, while the interval from 800 to 900 hPa affects it more above land than the water. Relatively speaking, the regional average contribution to dPW was 25% in the interval 900–1000 hPa and 45% in the next 100 hPa layer. The 800–1000 hPa interval describes 80% of the magnitude of PW’s diurnal cycle above the land, while above the sea its contribution is about 20% smaller.

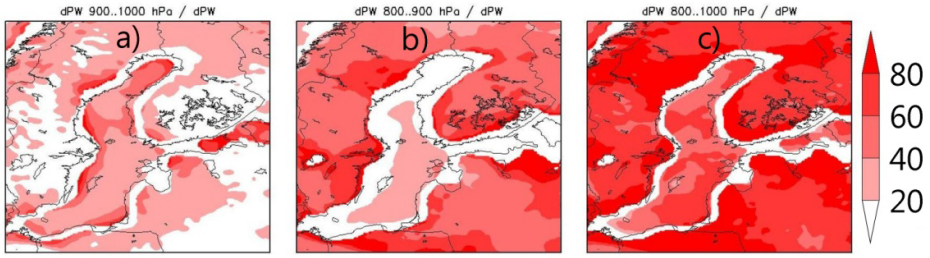


Figure 12. Contributions of different vertical intervals to precipitable water, PW, calculated as a PW difference between 18 and 06 UTC using data from BaltAn65+ for 1979–2005. Relative (%) contribution to PW difference from a respective vertical interval is given: a) 900–1000 hPa; b) 800–900 hPa; c) 800–1000 hPa. Regarding the diurnal variation in PW, the lowest vertical interval from 900 to 1000 hPa is the most important contributor above the water, while the cycle above the land is most affected by the next 100 hPa layer.

5. INTERCOMPARISONS BETWEEN TECHNIQUES AND MODELS

5.1. Intercomparisons in Estonia

5.1.1. The campaign from 22 June to 6 November 2008 at Tõravere

During the campaign from 22 June to 6 November 2008, the PW retrievals by AERONET, GPS and HIRLAM were available. These methods enabled to generate three different pairs with concurrent PW estimations. Methods were investigated in pairs for the purpose to find linear fits, coefficients of determination, mean bias differences (MBD) as well as root-mean-square differences (RMSD).

Fig. 13 illustrates the linear fits and correlations between GPS, AERONET and HIRLAM. The linear fit through zero, as an ideal relation in case of the value of the slope $a = 1$, was used. As can be seen from the Fig. 13a, the comparison of PW obtained with AERONET and GPS is best described with a regression:

$$PW(\text{AERONET}) = 0.96 PW(\text{GPS}) . \quad (5.1)$$

Examination of Fig. 13a shows that the differences between PW estimated by these methods are visually most notable at PW values below 12 mm (when AERONET evaluated PW somewhat higher than GPS) and above 25 mm (when AERONET underestimated PW compared to GPS). Regarding the linear fit, there is no physical reason to use an intercept, while every method should give us PW value of 0 mm if there is no water vapour in the air. However, adding an intercept to the regression we get:

$$PW(\text{AERONET}) = 0.89 PW(\text{GPS}) + 1.33 , \quad (5.2)$$

which is similar as the result drawn from the studies by Smirnov *et al.* (2004) and Cl  mer *et al.* (2008).

Fig. 13b compares the AERONET outputs with its HIRLAM counterparts. The linear regression for comparison between PW obtained with AERONET and HIRLAM is:

$$PW(\text{AERONET}) = 0.97 PW(\text{HIRLAM}) . \quad (5.3)$$

As can be seen from Fig. 13b, the data points are more scattered than in a previous comparison. This refers to the shortfall of HIRLAM to describe the variability of PW as accurately as GPS. Similar deviation of data from the best fit line becomes evident as was shown by comparison of PW values estimated by AERONET and GPS. The evidence suggests that compared to GPS,

AERONET overestimates PW by 5% at values below 12 mm and underestimates PW by 6% at values over 25 mm. Compared to HIRLAM, these numbers are 9% and 10%, respectively.

As revealed by Fig. 13c, the data points between PW(HIRLAM) and PW(GPS) are evenly scattered around the best fit line, but compared to previous relations, points are more dispersed. The relation between these methods can be described by a regression:

$$\text{PW(HIRLAM)} = 0.98 \text{ PW(GPS)} . \quad (5.4)$$

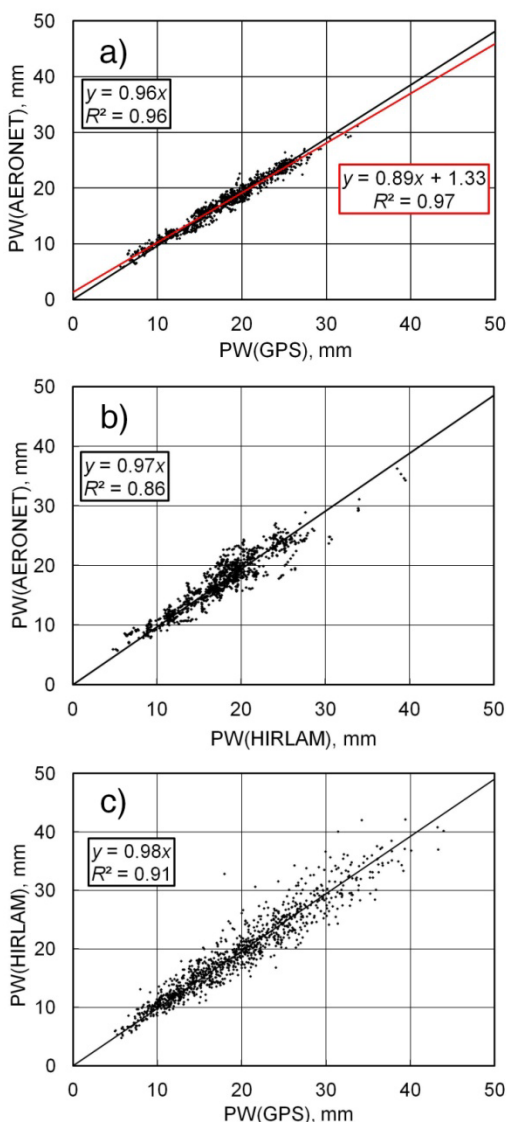


Figure 13. Comparison of estimations of precipitable water, PW, at Tõravere during the period from 22 June to 6 November 2008: a) AERONET vs. GPS, b) AERONET vs. HIRLAM, and c) HIRLAM vs. GPS. The linear fit and coefficient of determination, R^2 , are given on each panel. Compared to HIRLAM and GPS, AERONET-derived PW is slightly overestimated when its value is smaller than 12 mm and underestimated when its value is above 25 mm. The pairs involving HIRLAM show higher scatter from the linear fit because of relatively low temporal and spatial resolution of the model.

The campaign was also used to assess the uncertainty of techniques. According to the technical information about the barometer used in Tõravere, the uncertainty in pressure, $u(P_0) = 0.17$ hPa. Applying the Equation (2.20) for every single GPS measurement yields the average $u(\text{GPS}) = 1.2$ mm. In this experiment, the last value coincides with the average “formal error” (as a rough estimate of 1σ) calculated by the GAMIT software. The most comprehensive study made for Northern Europe, to compare PW time series from HIRLAM simulations with estimates from ground-based GPS receivers, was done by Yang *et al.* (1999). In the experiment, the overall average scatter of HIRLAM predictions, in regard to GPS, was characterized by the RMSD equal to 2.4 mm (18%). This result and the law of propagation of uncertainty is used for a rough calculation of uncertainty in PW simulations by HIRLAM:

$$\sqrt{u^2(\text{GPS}) + u^2(\text{HIRLAM})} = 2.4 \text{ mm}. \quad (5.5)$$

Inserting $u(\text{GPS}) = 1.2$ mm, we obtain that $u(\text{HIRLAM}) = 2.1$ mm. This, as a first approximation, is used in further calculations.

A consistency test using concept proposed by Immmler *et al.* (2010) was also carried out. The pair of datasets that involved AERONET showed extremely high rate (>87%) of “strong consistency” and very low “weak consistency” percents (0–1%) referring that the uncertainty in AERONET-estimated PW should be considerably smaller than the 10%, previously reported by Holben *et al.* (2001). Results of this campaign suggest the uncertainty in PW to be only about 3%.

Table 2 summarizes the results of the first study period.

Table 2. Slopes, a , for linear fits, $y = ax$, mean bias differences (MBD) and root-mean-square differences (RMSD) between three PW estimation methods at Tõravere, 22 June – 6 November 2008. The uncertainty of the slope is given at a 95% confidence level. Number of coupled observations is N .

Pair of methods	N	Slope, a	MBD	MBD%	RMSD	RMSD%
AERONET (y) vs GPS (x)	1038	0.96 ± 0.003	−0.5 mm	−2.2%	1.2 mm	6.7%
HIRLAM (y) vs GPS (x)	1057	0.98 ± 0.006	−0.2 mm	−0.2%	2.2 mm	11.3%
AERONET (y) vs HIRLAM (x)	1066	0.97 ± 0.006	−0.3 mm	−1.0%	1.8 mm	10.1%

5.1.2. The campaign from 9 to 12 August 2010 at Tõravere

For the short campaign, data obtained by four methods – radiosonde, AERONET, GPS, and HIRLAM – were available (Fig. 14). Keeping in mind a historical role of radiosonde in investigation of column humidity, it was

considered as a preliminary reference in this campaign. The soundings carried out by the Estonian Defence Forces using the GRAW DFM-06 sonde were not assimilated into the HIRLAM.

Comparing single PW estimates by different methods, discrepancies were unexpectedly large. The largest one, 9.1 mm, occurred on 12 August when the PW estimate by GPS was 37.3 mm, but by HIRLAM only 28.2 mm. However, no relationships between vertical humidity profiles and PW discrepancies were found. Positive as well as negative biases occurred for relatively similar profiles.

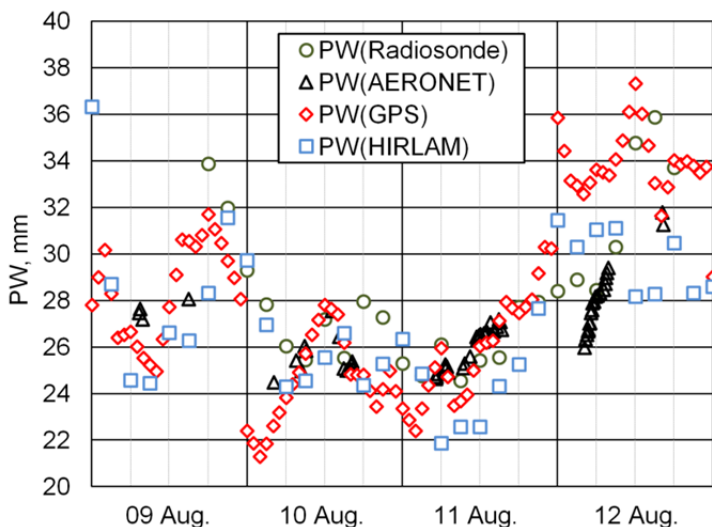


Figure 14. Evolution of PW estimated by four methods – radiosonde, AERONET, GPS, and HIRLAM – at Tõravere during the 2010 campaign.

GPS performed the closest values to radiosonde, being “drier”, MBD = -0.2 mm (-0.7%). In terms of the scatter from radiosonde, AERONET was the best method, RMSD = 1.7 mm (5.5%). With MBD = -0.6 mm (-1.7%), AERONET showed slightly higher systematic deviation from radiosonde compared to GPS. The largest average systematic deviation from radiosonde, towards “drier” estimations, was demonstrated by HIRLAM, MBD = -1.5 mm (-4.8%).

During the shorter campaign, the four different PW estimation methods enable to generate six different pairs. Intercomparison of their performance, in terms of the slope, MBD and RMSD, is given in Table 3.

Table 3. Slopes, a , for linear fits, $y = ax$, mean bias differences (MBD) and root-mean-square differences (RMSD) between four PW estimation methods at Tõravere, 9–12 August 2010. The uncertainty of the slope is given at a 95% confidence level. Number of coupled observations is N .

Pair of methods	N	Slope, a	MBD	MBD%	RMSD	RMSD%
HIRLAM (y) vs Radiosonde (x)	25	0.94 ± 0.04	–1.5 mm	–4.8%	3.0 mm	9.6%
GPS (y) vs Radiosonde (x)	25	0.99 ± 0.05	–0.2 mm	–0.7%	3.2 mm	11.1%
AERONET (y) vs Radiosonde (x)	11	0.97 ± 0.04	–0.6 mm	–1.7%	1.7 mm	5.5%
AERONET (y) vs GPS (x)	25	0.96 ± 0.04	–0.8 mm	–2.1%	2.6 mm	8.3%
HIRLAM (y) vs GPS (x)	25	0.94 ± 0.05	–1.3 mm	–3.2%	3.6 mm	12.7%
AERONET (y) vs HIRLAM (x)	11	1.02 ± 0.07	0.7 mm	3.9%	2.8 mm	11.0%

Checking the pairs of independent measurements for consistency with Equation (2.28), the highest consistency was determined in pairs which involved AERONET. In all these pairs – AERONET vs Radiosonde, AERONET vs GPS, HIRLAM vs AERONET – Equation (2.28) was true for $k = 1$ more than 79% of cases, justifying the data to be called “strongly consistent”. In addition, in pairs AERONET vs Radiosonde and HIRLAM vs AERONET, there was no individual case when the measurements were “weakly consistent” or “inconsistent” (Equation (2.28) not true for $k = 2$ and $k = 3$, respectively). Similarly to the longer campaign, the results confirm that the uncertainty in AERONET-derived PW is considerably less than reported by the AERONET team.

5.2. Validation of reanalyses over the Arctic

During the drift of the ice station Tara in the Central Arctic Ocean from 25 April to 31 August 2007, a total of 95 tethersonde soundings during 39 days were made using a Vaisala DigiCORA Tethersonde System (Fig. 15). These observations were not assimilated in any reanalyses. The sounding data was used to validate the NCEP-DOE, NCEP-CFSR, ERA-Interim, JCDAS, and MERRA reanalyses by means of observed temperature, specific humidity (SH) and relative humidity (RH) profiles. From the entire dataset collected during the campaign, 29 profiles reaching height up to 890 m were chosen for validation purposes.

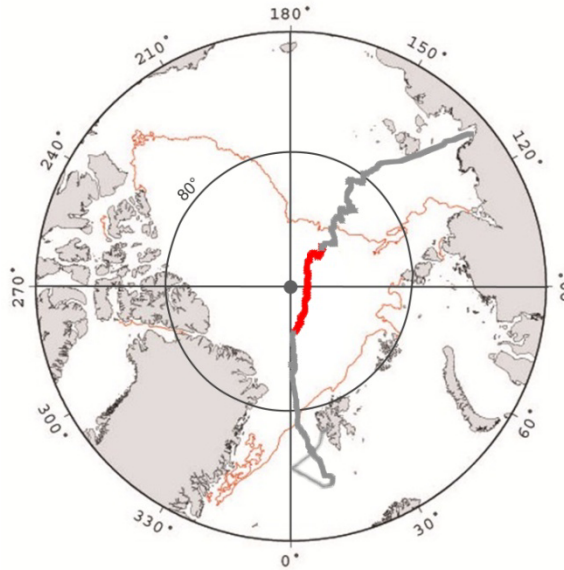


Figure 15. Drift trajectory of the ice station Tara (red) from the period of tethersonde soundings: 25 April to 31 August, 2007. The brown line shows the minimum sea ice extent in September.

Among the reanalyses, basically only ERA-Interim reproduced the shape of the SH profile, but with a significant moist bias of 0.3 to 0.5 g kg^{-1} throughout the profile, and missing the humidity inversion in the lowermost 180 m (Fig. 16). ERA-Interim RH had a significant moist bias of up to 9% in the whole profile. The observed mean SH profile was best captured by NCEP-CFSR, with mostly dry insignificant biases of up to 0.3 g kg^{-1} . The cold bias clearly dominated over the dry bias, seen as a mostly significant (i.e., significant at most measurement heights) wet bias in the RH of NCEP-CFSR. MERRA-derived SH had significant dry bias above 150 m with the magnitude increasing with altitude to 0.5 g kg^{-1} . Considering RH, MERRA had a mostly significant dry bias of approximately 6% in the whole profile. The mean SH profiles of JCDAS and NCEP-DOE showed a mostly significant moist bias in the lowermost 600 m and a strong decrease of air moisture upward of the height of $100\text{--}150 \text{ m}$. JCDAS had a mostly significant positive bias in RH but NCEP-DOE values almost perfectly matched the observations in the layer of 100 to 550 m . This was, however, due to the combined effects of warm and moist (in the sense of SH) bias.

Considering the RMSE in SH, NCEP-CFSR outperformed the other reanalyses in the whole profile (Fig. 16d), but for RH, none of the reanalyses were clearly better than the others (Fig. 16f). Except of the SH profile derived from JCDAS, the RMSE of SH and RH increased with height up to the altitude of at least 500 m .

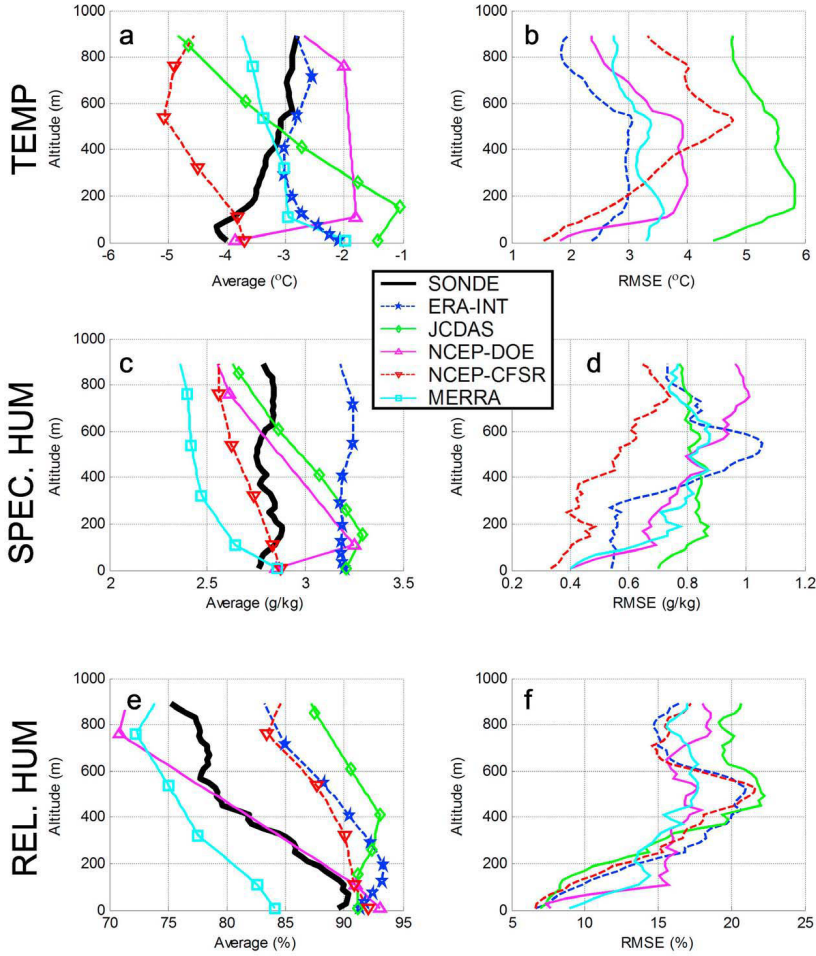


Figure 16. Vertical profiles of some meteorological parameters in the Arctic: (a) average temperature, (b) RMSE (root mean square error) of temperature, (c) average specific humidity, (d) RMSE of specific humidity, (e) average relative humidity and (f) RMSE of relative humidity calculated from 29 tethered sonde-measured single profiles and five reanalyses. The profile of specific humidity measured by the tethered sonde was best reproduced by NCEP-CFSR.

The summertime correlation coefficient r for SH (not shown) varied in NCEP-CFSR and ERA-Interim from 0.4 to 0.7. JCDAS had a minimum r of 0.2 and MERRA even below 0.1. The worst model was NCEP-DOE with a negative r down to -0.5 above the height of 250 m. Correlations for the RH were generally smaller than for the SH, r typically ranging from 0.2 to 0.6.

In the individual profiles of SH (not shown), ERA-Interim had the highest positive errors, even exceeding 3 g kg^{-1} . In three cases the observed SH was

approximately 2.5 g kg^{-1} , while the ERA-Interim SH was approximately 6 g kg^{-1} . All these cases were associated with a strong ($8 \text{ }^{\circ}\text{C}$) temperature inversion. In these cases the temperature profile was fairly well reproduced by ERA-Interim, but the reanalysis RH was excessive, close to a 100% compared to the observed 35 to 60%. The highest negative errors in SH, less than -2 g kg^{-1} , occurred in NCEP reanalyses, associated with strong ($8 \text{ }^{\circ}\text{C}$) temperature inversions that were not captured by the reanalyses.

A layer with a SH increase larger than 0.2 g kg^{-1} was considered as a humidity inversion. The measured 29 profiles included 21 cases with a humidity inversion, detecting 2.6 g kg^{-1} as the maximum inversion rate between nearby layers. NCEP-DOE captured 15 inversions and 4 false inversions. ERA-Interim captured 10 inversions and MERRA 9 inversions with no false inversions. NCEP-CFSR captured 7 inversions and 1 false inversion whereas JCDAS captured 4 inversions and 3 false inversions.

The observed biases in temperature and humidity are comparable or even larger than the climatological trends during the latest decades (Serreze *et al.*, 2009). This calls for caution when applying reanalysis data in climatological studies. However, regarding SH, if one reanalysis should be selected, NCEP-CFSR is recommended on the basis of this study.

6. CONCLUSIONS

6.1. The main findings

- Vaisala RS80-A, RS90 and RS92 radiosonde measurements performed in Estonia and Finland during 1998–2012 and 1982–2012, respectively, indicated that troposphere has become warmer at all altitudes up to 7 km, $0.3\text{--}1.0\text{ }^{\circ}\text{C (10 yr)}^{-1}$, and more moist below the altitude of 2 km, $3\text{--}5\% (10\text{ yr})^{-1}$. Nevertheless, annual trends in specific humidity (SH) and temperature in all of the stations are relatively small, if statistically significant at all. Therefore, trends in annual precipitable water, PW, were not found.
- Monthly trends in SH up to the altitude of 7 km differ from station to station and are inhomogeneous for different altitudes and months. Precipitable water and North Atlantic Oscillation (NAO) index are significantly related during the winter period (December, January, February) at all four stations studied in Finland and Estonia, coefficient of correlation, r , ranging from 0.47 to 0.55. Correlation between monthly SH values and NAO index is strongest in January, February and March, especially below 2 km level, where correlation coefficients reach up to 0.8.
- Derived from a deficient calibration model, a significant dry bias in Vaisala RS80-A humidity measurements at temperatures $<-20\text{ }^{\circ}\text{C}$ is notable. To eliminate this bias, a correction proposed by Leiterer *et al.* (2005) was used. The impact of the correction on specific humidity increases with height, rising yearly tropospheric SH values by 3–20%. By increasing SH values at all altitudes throughout the troposphere, the correction changed the values of the trends at three Finnish stations towards negative values by 2–3% $(10\text{ yr})^{-1}$ and increased annual PW by about 4%. Based on the fact that the correction has a significant effect on atmospheric humidity, datasets retrieved by RS80-A and newer Vaisala radiosondes should not be united without homogenizing.
- The diurnal cycle of PW depends on whether the area of investigation is located above the Baltic Sea and larger lakes, or above the land. Humidity content above the water reaches a peak and decreases to the minimum at 00 UTC and 18 UTC, respectively. Above the land the peak is reached at 18 UTC and the minimum is detected at 06 UTC. The most important layer responsible for diurnal PW cycle above the water lies between 900 and 1000 hPa, while above the land it lies between 800 and 900 hPa.
- Apparently, based on intercomparisons of different PW estimation techniques carried out at Tõravere, Estonia, the most accurate alternative estimation method of PW to radiosonde is GPS. The GPS-measured PW is clean from obvious systematic effects and is also closest to radiosonde.
- A slight deviation of AERONET-derived PW became evident. Compared to the data from HIRLAM and GPS, AERONET overestimated PW by 5–9%

at values below 12 mm, and underestimated PW by 6–10% at values above 25 mm. Despite that, results suggest that the uncertainty in the AERONET-estimated PW is only about 3%, which is considerably less than previously reported by the AERONET team.

- Comparisons carried out at Tõravere indicated that a regional model HIRLAM can not compete by means of PW estimating precision against methods which use real-time measurements, if these measurements are not assimilated into the model. Comparing methods in pairs, the RMSD value involving HIRLAM is almost twice as large as between AERONET and GPS.
- Based on a validation carried out in the Arctic using measurements performed by a tethered sonde as a reference, NCEP-CFSR, NCEP-DOE, and MERRA reanalyses outperform JCDAS and ERA-Interim with respect to 2-m air temperature and SH. The whole vertical profile of SH up to 890 m was captured best by NCEP-CFSR, being the most reliable global model for estimating humidity in the lower troposphere.

6.2. Pathways for further research

During the course of the work presented in this thesis, topics for further research have arisen. Collection of issues to be concentrated on in the future involves the following:

- Apparently, the most promising method to estimate PW and its diurnal variations is GPS. However, there are datasets of GPS-derived PW waiting to be calculated in Estonia from four stations belonging to the European Reference Frame Permanent Network (EPN, 2015): Tõravere, Kuressaare, Toila and Suurupi. Intercomparison between AERONET and GPS in Tõravere can be extended from 2008 to the present, while GPS record in Suurupi dates back to 1996, offering the opportunity to compare it with radiosonde data from the nearby site Harku.
- Homogenisation of radiosonde records is an important aspect when investigating long-term trends and variability in humidity. Regarding the only radiosonde site in Estonia, Harku, the sondes produced in France by MeteoModem (MeteoModem, 2015) are in use since 1 July 2013 replacing the Vaisala sondes. Every break in homogeneity (e.g. derived from a change in the sonde type) suggests the need to correct one of the humidity records retrieved by the same type of sonde. After some time, even a dataset derived by the newest sonde type available may need a correction if comparisons with reference techniques or laboratory experiments have proved this kind of necessity.
- Satellite remote sensing of the atmosphere is considered to estimate the PW with high spatial resolution and accuracy over land surfaces for cloud-free conditions. Ocean and Land Color Instrument (OLCI) on the board of

Sentinel-3, suitable for this purpose, will be probably launched during 2015. In addition, measurements in the near infrared from MODIS (MODerate Resolution Imaging Spectroradiometer) mounted on both polar orbiting Earth Observing System platforms, Terra and Aqua, enable to retrieve PW above land since 1999 (Gao and Kaufman, 2003). However, the accuracy of the MODIS retrieval was not sufficient until recently, when Diedrich *et al.* (2014) improved it considerably. This work has led to considerable decrease in uncertainty of MODIS, now estimated to be only 2–3%. On the other hand, water vapour remote sensing over oceans is carried out since the 1980s with microwave radiometers (e.g. with SSM/I: Schluessel and Emery, 1990), but with low spatial resolution. It should be noted that except the JRA-25, a reanalysis developed by the Japan Meteorological Agency, PW over the oceans derived from SSM/I is not an input to any of the reanalyses. Moreover, none of the reanalyses takes into account PW derived from satellites over land, offering the opportunity to validate reanalyses against satellites.

SUMMARY IN ESTONIAN

“Atmosfääri niiskussisaldus – määramismeetodid ning muutlikkus Läänemere piirkonnas ja Arktikas”

Kuna veeauru ruumiline jaotumine mõjutab otseselt sademete ja pilvede teket, keemilisi reaktsioone ning kiirguslevi atmosfääris, on see oluline nii hetkeilma kui kliima kujundaja. Omades mudelennustuste põhjal suurimat positiivset tagasimõju kliima soojenemisele, on veeauru ühtlustatud aegridadel kliimauuringutes suur tähtsus.

Veeauru, kui kõige olulisema kasvuhoonegaasi mõõtmisel on endiselt suuri maks probleemiks selle ajalise ja ruumilise muutlikkuse kirjeldamine. Seda isegi hoolimata viimastel aastakümnetel lisandunud meetoditest nagu GPS- ja satelliitmeteoroloogia, mis nüüd on kasutusel kõrvuti traditsioonilisemate atmosfääri niiskussisalduse määramisviisidega nagu raadiosond. Lisaks sellele on numbriliste ilmaennustusmodelite ja järelanalüüsides andmebaasid osutunud olulisteks abivahenditeks atmosfääri seisundi muutuste hindamisel, seda eriti piirkondades, kus mõõtmisvõrgustik on puudulik (näiteks mered, suured järved, polaar- ja mägised alad). Kuigi atmosfääri niiskussisalduse määramisviise on mitmeid, pole neist veel ühtki seatud etalonmeetodi staatusesse. See tekitab jätkuva vajaduse viia läbi võrdluskatseid, mis aitavad selgitada välja meetodite täpsuse, tugevused ja nõrkused.

Pöörates peatähelepanu sadestatavale veeaurule (*precipitable water*, PW), mille väärtus on võrdne veekihi paksusega, kui atmosfäärisambas olev veeaur kondenseerida, ja sellega seotud karakteristikule, eriniiskusele (SH), on doktoritöös neli suuremat eesmärki:

- 1) uurida atmosfääriniiskuse pikaajalist muutlikkust ja trende erinevatel kõrgusnivoodel, kasutades Vaisala Oy raadiosondide RS80-A, RS90 ja RS92 aegridasid, mis pärinevad ühest Eesti ja kolmest Soome raadiosondeerimisjaamast;
- 2) selgitada PW suvist ööpäevast käiku Läänemere piirkonnas, uurides aastate 1979–2005 andmeid, mis pärinevad kahest järelanalüüsist: NCEP-CFSR (USA) ja BaltAn65+;
- 3) hinnata Eestis kasutusel olevate PW määramismeetodite (raadiosondeerimine, AERONET, GPS, HIRLAM) täpsust ja, kasutades Tõraveres teostatud kahe võrdluskampaania tulemusi, soovitada alternatiivne meetod raadiosondile, mida on ajalooliselt peetud täpseimaks;
- 4) valideerida 2007. aastal Arktikas läbi viidud nöörsondeerimiste põhjal viit levinuimat järelanalüüsi andmebaasi (ERA-Interim, NCEP-CFSR, NCEP-DOE, JCDAS, MERRA) atmosfääriniiskuse määramisel aluspinnalähedases (1 km) kihis.

Doktoritöö tulemused:

- Eestis ja Soomes kogutud raadisondeerimisandmed näitavad, et kuni 7 km ulatuses on, vastavalt perioodidel 1998–2012 ja 1982–2012, aset leidnud soojenemine, $0.3\text{--}1.0\text{ }^{\circ}\text{C (10 yr)}^{-1}$. Maapinnalähedases 2 km kihis on täheldatav ka niiskussisalduse kasv, $3\text{--}5\% (10\text{ yr})^{-1}$. Siiski, isegi kui pikaajaliselt temperatuuri ja niiskussisalduse trendid erinevatel nivoodel on statistiliselt usaldusväärsed, on need trendid enamasti väikesed. Seetõttu trende nelja jaama PW aastakeskmistes väärtustes ei ilmne.
- Eriniiskuse kuutrendid on uuritud raadisondeerimisjaamades kõrguste ja kuude lõikes erinevad. Kõikides jaamades on PW ja Põhja-Atlandi Ost-sillatsiooni (NAO) indeksi vahel tuvastatav statistiliselt usaldusväärne seos talvel (detsember, jaanuar, veebruar), mil korrelatsioonikoefitsient, $r = 0.47\text{--}0.55$. Eriniiskuse ja NAO indeksi kuukeskmiste väärtuste vahel on tugevaim korrelatsioon täheldatav madalamal kui 2 km jaanuaris, veebruaris ja märtsis, mil korrelatsioonikoefitsiendi väärtus on kuni 0.8. Seetõttu, suhteliselt soojemad ja niiskemad talved on põhjustatud intensiivsematest lääne- ja edelasuunalistest Atlandilt pärit tuultest.
- Tulenevalt ebatäpsest kalibratsioonimudelist, ilmneb Vaisala RS80-A sondi mõõtmistes oluline niiskuse alahindamine madalamatel temperatuuridel kui $-20\text{ }^{\circ}\text{C}$. Alahindamise kõrvaldamiseks kasutatud korrektsiooni mõju eriniiskuse väärtusele kasvab kõrgusega. Korrektsioon suurendab troposfääri ulatuses eriniiskuse väärtusi $3\text{--}20\%$ ning seetõttu muudab kolmes uuritud Soome raadisondeerimisjaamas eriniiskuse trende $2\text{--}3\% (10\text{ yr})^{-1}$ negatiivsemate väärtuste suunas. Kuna Vaisala RS80-A niiskuse korrektsioonil on oluline mõju atmosfääri niiskussisalduse väärtusele, ei tohiks RS80-A ja uuemate sondidega saadud niiskuse aegridasid ilma ühtlustamata omavahel ühendada.
- Õhusamba niiskussisalduse PW ööpäevane käik suvel sõltub aluspinnast. Läänemere piirkonnas saavutab see käik mere ja suuremate järvede kohal maksimumi kell 00 ja miinimumi kell 18 UTC. Võrreldes käiguga suuremate veekogude kohal, on ööpäevane käik maa kohal ümberpööratud, omades maksimumi kell 18 UTC ja miinimumi kell 06 UTC. Õhusamba niiskussisalduse PW ööpäevane muutlikkus vee kohal on tingitud peamiselt muutustest atmosfäärikihis, mis paikneb 900 ja 1000 hPa vahel (allpool 1 km). Maapinna kohal tuleneb PW ööpäevane muutlikkus peamiselt kihist, mis paikneb 800 ja 900 hPa vahel (1–2 km).
- Tõraveres teostatud võrdluskampaaniate tulemused viitavad sellele, et PW määramisel on Eestis kasutusel olevatest meetoditest parim alternatiiv raadisondile GPS-meetod.
- Võrreldes GPS-meetodiga ja regionaalse ilmaennustusmudeliga HIRLAM, ülehindab AERONET päikesefotomeeter PW väärtust $5\text{--}9\%$, kui selle väärtus on väiksem kui 12 mm, ja alahindab $6\text{--}10\%$, kui selle väärtus on suurem kui 25 mm. Sellegipoolest, AERONET'i mõõdetud PW määramatus

on võrdlusmõõtmiste põhjal vaid 3%, mis on tunduvalt vähem, kui varem hinnatud AERONET'i meeskonna poolt.

- Regionaalne ilmaennustusmudel HIRLAM ei suuda hinnata PW väärtust sama täpselt kui meetodid, mis kasutavad vaadeldavas jaamas konkreetseid mõõtmistulemusi, kui need mõõtmistulemused ei ole mudeli sisendiks.
- Tuginedes temperatuuri- ja niiskusandmetele, mis saadi nööri sondiga mõõtmisel Arktikas 2007. aasta suvel, suudavad viiest võrreldud järelanalüüsist kõige täpsemini hinnata 2-m õhutemperatuuri ja eriniiskust NCEP-CFSR, NCEP-DOE ja NASA MERRA. Seevastu eriniiskuse profiil, mis ulatus võrdlustes kuni 890 m kõrguseni, on kõige paremini kirjeldatud NCEP-CFSR järelanalüüsi andmetega.

REFERENCES

- AERONET (2015). <http://aeronet.gsfc.nasa.gov/>, retrieved 28 January 2015.
- Alduchov, O. A., Eskridge, R. E. (1996). Improved Magnus form approximation of saturation vapor pressure. *J. Appl. Meteor.*, **35**, 601–609.
- Antikainen, V., Paukkunen, A. (1994). Studies on improving humidity measurements in radiosondes. *Instruments and observing methods*, 137–141, WMO, Geneva.
- Aruksaar, H., Liidemaa, H., Martin, I., Mürk, H., Nei, I., Põiklik, K. (1964). *Üld- ja agrometeoroloogia (General and Agrometeorology)*. Eesti Raamat: Tallinn.
- Askne, J. and Nordius, H. (1987). Estimation of tropospheric delay for microwaves from surface weather data. *Radio Sci.*, **22**, 379–386.
- August, E. F. (1828). Ueber die Berechnung der Expansivkraft des Wasserdunstes. *Ann. Phys. Chem.*, **13**, 122–137.
- Bengtsson, L., Robinson, G., Anthes, R., Aonashi, K., Dodson, A., Elgered, G., Gendt, G., Gurney, R., Jietai, M., Mitchell, C., Mlaki, M., Rhodin, G., Silverstrin, P., Ware, R., Watson, R., Wergen, W. (2003). The use of GPS measurements for water vapor determination. *Bull. Am. Meteorol. Soc.*, **84**, 1249–1258.
- Bevis, M., Businger, S., Herring, T. A., Rocken, C., Anthes, R. A., Ware, R. H. (1992). GPS meteorology: Remote sensing of atmospheric water vapor using the Global Positioning System. *J. Geophys. Res.*, **97**, 15787–15801.
- Bosilovich, M. G., Kennedy, J., Dee, D., Allan, R., O'Neill, A. (2013). On the reprocessing and reanalysis of observations for climate. In: *Climate Science for Serving Society: Research, Modelling and Prediction Priorities*, edited by G. Asrar and J. Hurrell, Springer Science+Business Media Dordrecht, doi: 10.1007/978-94-007-6692-1_3.
- Bouma, H. R., Stoew, B., (2001). GPS observations of daily variations in the atmospheric water vapor content. *Phys. Chem. Earth*, **26** (A6-8), 389–392.
- Bouma, H. R. (2002). *Ground-based GPS in climate research*. Tech. Rep. No. 456L, Licentiate Thesis, School Environ. Sci. School Electric. Eng., Chalmers Univ. of Tech., Göteborg.
- Cady-Pereira, K. E., Shephard, M. W., Turner, D. D., Mlawer, E. J., Clough, S. A., Wagner, T. J. (2008). Improved daytime column-integrated precipitable water vapor from Vaisala radiosonde humidity sensors. *J. Atmos. Ocean. Tech.*, **25**, 873–883.
- Cole, H., Miller, E. (1995). A correction for low-level radiosonde temperature and relative humidity measurements. Preprints, *Ninth Symp. on Meteorological Observations and Instrumentation*, Charlotte, NC, Amer. Meteor. Soc., 32–36.
- Cullather, R. I., Bosilovich, M. G. (2011). The moisture budget of the polar atmosphere in MERRA. *J. Clim.*, **24**, 2861–2879, doi:10.1175/2010JCLI4090.1.
- Dai, A., Giorgi, F., Trenberth, K. E. (1999a). Observed and model-simulated precipitation diurnal cycle over the contiguous United States. *J. Geophys. Res.*, **104** (D6), 6377–6402, <http://dx.doi.org/10.1029/98JD02720>.
- Dai, A., Trenberth, K. E., Karl, T. R. (1999b). Effects of clouds, soil moisture, precipitation and water vapor on diurnal temperature range. *J. Climate*, **12** (8), 2451–2473, [http://dx.doi.org/10.1175/15200442\(1999\)012<2451:EOCSMP>2.0.CO;2](http://dx.doi.org/10.1175/15200442(1999)012<2451:EOCSMP>2.0.CO;2).
- Dai, A., Wang, J., Ware, R., Van Hove, T. (2002). Diurnal variation in water vapor over North America and its implications for sampling errors in radiosonde humidity. *J. Geophys. Res.*, **107** (D10), ACL 11-1–ACL 11-14, <http://dx.doi.org/10.1029/2001JD000642>.

- Dai, A. (2006). Recent climatology, variability, and trends in global surface humidity. *J. Climate*, **19**, 3589–3606.
- Dee, D. P., et al. (2011). The ERA-Interim reanalysis: Configuration and performance of the data assimilation system. *Q. J. R. Meteorol. Soc.*, **137**, 553–597, doi:10.1002/qj.828.
- Diedrich, H., Preusker, R., Lindstrot, R., Fischer, J. (2014). Retrieval of daytime total columnar water vapour from MODIS measurements over land surfaces. *Atmos. Meas. Tech. Discuss.*, **7**, 7753–7792, doi:10.5194/amtd-7-7753-2014.
- Durre, I., Williams Jr., C. N., Yin, X., Vose, R. S. (2009). Radiosonde-based trends in precipitable water over the Northern Hemisphere: An update. *J. Geophys. Res.*, **114**, D05112, doi:10.1029/2008JD010989.
- Emardson, T. R., Elgered, G., Johansson, J. M. (1998). Three months of continuous monitoring of atmospheric water vapor with a network of Global Positioning System receivers. *J. Geophys. Res.*, **103**, 1807–1820.
- [EM] Earth Magazine (2012). Arctic humidity on the rise. *Earth Magazine*, 07 October 2012. <http://www.earthmagazine.org/article/arctic-humidity-rise>, retrieved 10 March 2015.
- [EU FAC] EU Foreign Affairs Council (2014). Foreign Affairs Council meeting, Brussels, 12 May 2014. http://www.consilium.europa.eu/uedocs/cms_Data/docs/pressdata/EN/foraff/142554.pdf, retrieved 10 March 2015.
- [EPN] The European Reference Frame Permanent Network (2015). <http://www.epncb.oma.be/>, retrieved 28 January 2015.
- Fowle, F. E. (1912). The spectroscopic determination of aqueous vapor. *Astrophys. J.*, **35**, 149–162.
- Gaffen, D. J., Elliott, W. P., Robock, A. (1992). Relationships between tropospheric water vapor and surface temperature as observed by radiosondes. *Geophys. Res. Lett.*, **19**, 1839–1842.
- Gao, B.-C., Kaufman, Y. J. (2003). Water vapor retrievals using Moderate Resolution Imaging Spectroradiometer (MODIS) near-infrared channels, *J. Geophys. Res.-Atmos.*, **108**, 4389, doi:10.1117/12.154909, 2003.
- [GCOS] Global Climate Observing System (2010). *Guideline for the Generation of Datasets and Products Meeting GCOS Requirements*, <http://www.wmo.int/pages/prog/gcos/Publications/gcos-143.pdf>, retrieved 28 January 2015.
- GRAW (2013). <http://www.graw.de/home/products2/radiosondes0/dfm-060/>, retrieved 11 December 2013.
- Halthore, R. N., Eck, T. F., Holben, B. N., Markham, B. L. (1997). Sun photometric measurements of atmospheric water vapor column abundance in the 940-nm band. *J. Geophys. Res.*, **102**, 4343–4352.
- Held, I. M., Soden, B. J. (2000). Water vapor feedback and global warming. *Annu. Rev. Energy Environ.*, **25**, 441–475.
- Herring, T. A. (1992). Modelling atmospheric delays in the analysis of space geodetic data. *Symposium on Refraction of Transatmospheric Signals in Geodesy*, Netherlands Geod. Commis. Ser. 36, edited by J. C. DeMunk and T. A. Spoelstra, 157–164, Ned. Comm. voor Geod., Delft.
- Hyland, R. W., Wexler, A. (1983). Formulations for the thermodynamic properties of the saturated phases of H₂O from 173.15 K to 473.15 K. *ASHRAE Trans.*, **89**(2A), 500–519.

- Immmler, F. J., Dykema, J., Gardiner, T., Whiteman, D. N., Thorne, P. W., Vömel, H. (2010). Reference Quality Upper-Air Measurements: guidance for developing GRUAN data products. *Atm. Meas. Tech.*, **3**, 1217–1231.
- Jakobson, E. (2009). Spatial and temporal variability of atmospheric column humidity. *Diss. Geophys. Univ. Tartu.*, **23**, Tartu University Press.
- Kanamitsu, M., Ebisuzaki, W., Woollen, J., Yang, S.-K., Hnilo, J. J., Fiorino, M., Potter, G. L. (2002). NCEP-DOE AMIP-II Reanalysis (R-2). *Bull. Am. Meteorol. Soc.*, **83**, 1631–1643, doi:10.1175/BAMS-83-11-1631.
- Keevallik, S. (2003). Changes in spring weather conditions and atmospheric circulation in Estonia (1955–95). *Int. J. Climatol.*, **23**, 263–270.
- Keevallik, S., Krabbi, M. (2011). Temperature, humidity and wind from Estonian and Finnish radiosonde data (1993–2009). *Estonian Journal of Engineering*, **17**, 4, 345–358, doi: 10.3176/eng.2011.4.05.
- Kämpfer, N. (2013). Introduction. *Monitoring Atmospheric Water Vapour*, edited by N. Kämpfer, ISSI Scientific Report Series 10, ISBN 978-1-4614-3908-0, Springer Science+Business Media.
- Law, K. S., Stohl, A., Quinn, P. K., Brock, C. A., Burkhardt, J. F., Paris, J.-D., Ancellet, G., Singh, H. B., Roiger, A., Schlager, H., Dibb, J., Jacob, D. J., Arnold, S. R., Pelon, J., Thomas, J. L. (2014). Arctic air pollution. New insights from POLARCAT-IPY. *Bull. Am. Meteorol. Soc.*, **95**, 1873–1895, doi:10.1175/BAMS-D-13-00017.1.
- Lawrence, M. G. (2005). The relationship between relative humidity and the dewpoint temperature in moist air: a simple conversion and applications. *Bull. Amer. Meteor. Soc.*, **86**, 225–233.
- Leiterer, U., Dier, H., Naeber, T. (1997). Improvements in radiosonde humidity profiles using RS80/RS90 radiosondes of Vaisala. *Contrib. Atmos. Phys.*, **70**, 319–336.
- Leiterer, U., Dier, H., Naeber, T. (1998). Improvements in radiosonde humidity profiles using RS80/RS90 radiosondes of Vaisala. *Proc. WMO Technical Conf. on Meteorological and Environmental Instruments and Methods of Observation (TECO-98)*, Casablanca, Morocco, WMO Instruments and Observing Methods Rep. 70, WMO/TD-No. 877, 215–219.
- Leiterer, U., Dier, H., Nagel, D., Naeber, T., Althausen, D., Franke, K., Katz, A., Wagner, F. (2005). Correction method for RS80-A Humicap humidity profiles and their validation by lidar backscattering profiles in tropical cirrus clouds. *J. Atmos. Ocean. Tech.*, **22**, 18–29.
- McCarthy, M. P., Thorne, P. W., Titchner, H. A. (2009). An analysis of tropospheric humidity trends from radiosondes. *J. Climate*, **22**, 5820–5838.
- Magnus, G. (1844). Versuche über die Spannkkräfte des Wasserdampfs. *Ann. Phys. Chem.*, **61**, 225–247.
- Mattar, C., Sobrino, J. A., Julien, Y., Morales, L. (2011). Trends in column integrated water vapour over Europe from 1973 to 2003. *Int. J. Climatol.*, **31**, 1749–1757.
- MeteoModem, (2015). <http://www.meteomodem.com/>, retrieved 28 January 2015.
- Miloshevich, L. M., Vömel, H., Paukkunen, A., Heymsfield, A., Oltmans, S. J. (2001). Characterization and correction of relative humidity measurements from Vaisala RS80-A radiosondes at cold temperatures. *J. Atmos. Ocean. Tech.*, **18**, 135–156.
- Miloshevich, L. M., Paukkunen, A., Vömel, H., Oltmans, S. J. (2004). Development and validation of a time lag correction for Vaisala radiosonde humidity measurements. *J. Atmos. Ocean. Tech.*, **21**, 1305–1327.
- Miloshevich, L. M., Vömel, H., Whiteman, D. N., Lesht, B. M., Schmidlin, F. J., Russo, F. (2006). Absolute accuracy of water vapor measurements from six operational

- radiosonde types launched during AWEX-G and implications for AIRS validation. *J. Geophys. Res.*, **111**, D09S10, doi:10.1029/2005JD006083.
- Ning, T. (2012). *GPS meteorology: With focus on climate application*. Göteborg, Chalmers University of Technology. Diss. ISBN/ISSN: 978-91-7385-675-1.
- [NOAA] National Oceanic and Atmospheric Administration (2014). <http://www.cpc.ncep.noaa.gov/products/precip/CWlink/pna/nao.shtml>, retrieved 11 February 2014.
- Okulov, O., Ohvri, H., Kivi, R. (2002). Atmospheric precipitable water in Estonia, 1990–2001. *Boreal Env. Res.*, **7**, 291–300. ISSN 1239-6095.
- Okulov O., Ohvri H., (2010). Column transparency and precipitable water in Estonia. *Variability during the last decades*, Lambert Acad. Publ., Saarbrücken, 69 pp.
- Onogi, K., et al. (2007). The JRA-25 Reanalysis. *J. Meteorol. Soc. Jpn.*, **85**, 369–432, doi:10.2151/jmsj.85.369.
- Ortiz de Galisteo, J. P., Cachorro, V., Toledano, C., Torres, B., Laulainen, N., Bennouna, Y., de Frutos, A. (2011). Diurnal cycle of precipitable water vapor over Spain. *Q. J. Roy. Meteor. Soc.*, **137** (657), 948–958, <http://dx.doi.org/10.1002/qj.811>.
- Paukkunen, A. (1995). Sensor heating to enhance reliability of radiosonde humidity measurement. *Proc. of 11th AMS Conference*, Dallas, 103–106.
- Paukkunen, A. (1998). New calibration procedure optimizes RS90 radiosonde performance. *Vaisala News*, 147.
- Paukkunen, A., Antikainen, V., Jauhiainen, H. (2001). The accuracy and performance of the new Vaisala RS90 radiosonde in operational use. Preprints, *11th Symp. on Meteorological Observations and Instrumentation*, Albuquerque, NM, Amer. Meteor. Soc., 98–103.
- Pérez-Ramírez, D., Whiteman, D. N., Smirnov, A., Lyamani, H., Holben, B. N., Pinker, R., Andrade, M., Alados-Arboledas, L. (2014). Evaluation of AERONET precipitable water vapour versus microwave radiometry, GPS, and radiosondes at ARM sites. *J. Geophys. Res.*, **119**, 9596–9613, doi: 10.1002/2014JD021730.
- Ross, R. J., Elliott, W. P. (2001). Radiosonde-based Northern Hemisphere tropospheric water vapor trends. *J. Clim.*, **14**, 1602–1611.
- Saastamoinen, J. (1972). Atmospheric correction for the troposphere and stratosphere in radio ranging of satellites. *The Use of Artificial Satellites for Geodesy, Geophys. Monogr. Ser.*, **15**, edited by S. W. Henriksen et al., 247–251, AGU, Washington, D.C.
- Saha, S., et al. (2010). The NCEP Climate Forecast System Reanalysis. *Bull. Am. Meteorol. Soc.*, **91**(8), 1015–1057, doi:10.1175/2010BAMS3001.1.
- Schluessel, P., Emery, W. J. (1990). Atmospheric water vapour over oceans from SSM/I measurements. *Int. J. Remote Sens.*, **11**, 753–766.
- Schmid, B., Michalsky, J. J., Slater, D. W., Barnard, J. C., Halthore, R. N., Liljegren, J. C., Holben, B. N., Eck, T. F., Livingston, J. M., Russell, P. B., Ingold, T., Slutsker, I. (2001). Comparison of columnar water-vapor measurements from solar transmittance methods. *Appl. Opt.*, **40**, 12, 1886–1896.
- Serreze, M. C., Barrett, A. P., Stroeve, J. C., Kindig, D. N., Holland, M. M. (2009). The emergence of surface-based Arctic amplification. *Cryosphere*, **3**, 11–19, doi:10.5194/tc-3-11-2009.
- Sherwood, S., Roca, R., Weckwerth, T. M., Andronova, N. G. (2010). Tropospheric water vapor, convection, and climate. *Rev. Geophys.*, **48**, (RG2001), doi:10.1029/2009RG000301.
- Smirnov, A., Holben, B. N., Lyapustin A., Slutsker, I., Eck, T. F. (2004). AERONET processing algorithms refinement. *AERONET Workshop*, May 10–14, El Arenosillo, Spain.

- Smit, H., Kivi, R., Vömel, H., Paukkunen, A. (2013). Thin film capacitive sensors. *Monitoring Atmospheric Water Vapour*, edited by N. Kämpfer, ISSI Scientific Report Series 10, ISBN 978-1-4614-3908-0, Springer Science +Business Media.
- Solomon, S., Rosenlof, K., Portmann, R., Daniel, J., Davis, S., Sanford, T., Plattner, G.-K. (2010). Contributions of stratospheric water vapour to decadal changes in the rate of global warming. *Science*, **327**, 1219–1223.
- Sonntag, D. (1994). Advancements in the field of hygrometry. *Meteor. Z.*, **3**, 51–66.
- Suortti, T., Kats, A., Kivi, R., Kämpfer, N., Leiterer, U., Miloshevich, L., Neuber, R., Paukkunen, A., Ruppert, P., Vömel, H., Yushkov, V. (2008). Tropospheric comparisons of Vaisala radiosondes and balloon-borne frost-point and Lyman- α hygrometers during the LAUTLOS-WAVVAP experiment. *J. Atmos. Ocean. Tech.*, **25**, 149–166, doi:10.1175/2007JTECHA887.1.
- Trenberth, K. E., Fasullo, J., Smith, L. (2005). Trends and variability in column-integrated atmospheric water vapor. *Climate Dyn.*, **24**, 741–758, doi:10.1007/s00382-005-0017-4.
- Trenberth, K. E., Jones, P. D., Ambenje, P., Bojariu, R., Easterling, D., Klein Tank, A., Parker, D., Rahimzadeh, F., Renwick, J. A., Rusticucci, M., Soden, B., Zhai, P. (2007). Observations: surface and atmospheric climate change. In: *Climate Change 2007: The Physical Science Basis*. Contribution of Working Group I to the Fourth Assessment Report of the Intergovernmental Panel on Climate Change [Solomon, S., Qin, D., Manning, M., Chen, Z., Marquis, M., Averyt, K. B., Tignor, M., Miller, H. L. (eds.)]. Cambridge University Press, Cambridge, United Kingdom and New York, NY, USA.
- Tuomenvirta, H. (2004). Reliable estimation of climatic variations in Finland. *Contributions*, **43**, Finnish Meteorological Institute, 82 pp.
- Vaisala (2012). <http://www.vaisala.fi/Vaisala%20Documents/Technology%20Descriptions/HUMICAP-Technology-description-B210781EN-C.pdf/>, retrieved 28 January 2015.
- Van Baelen, J., Aubagnac, J.-P., Dabas, A. (2005). Comparison of near-real time estimates of integrated water vapor derived with GPS, radiosondes, and microwave radiometer. *J. Atmos. Ocean. Tech.*, **22**, 201–210.
- Vömel, H., Selkirk, H., Miloshevich, L., Valverde-Canossa, J., Valdes, J., Kyrö, E., Kivi, R., Stolz, W., Peng, G., Diaz, J. A. (2007a). Radiation dry bias of the Vaisala RS92 humidity sensor. *J. Atmos. Ocean. Tech.*, **24**, 953–963, doi:10.1175/JTECH2019.1.
- Vömel, H., David, D. E., Smith, K. (2007b). Accuracy of tropospheric and stratospheric water vapor measurements by the cryogenic frost point hygrometer: Instrumental details and observations. *J. Geophys. Res.*, **112**, D08305, doi:10.1029/2006JD007224.
- Wang, J., Cole, H. L., Carlson, D. J., Miller, E. R., Beierle, K., Paukkunen, A., Laine, T. K. (2002). Corrections of humidity measurement errors from the Vaisala RS80 radiosonde – application to TOGA COARE data. *J. Atmos. Ocean. Tech.*, **19**, 981–1002.
- Wang, J., Zhang, L. (2008). Systematic errors in global radiosonde precipitable water data from comparisons with ground-based GPS measurements. *J. Clim.*, **21**, 2218–2238, doi:10.1175/2007JCLI1944.1.
- Wexler, A. (1976). Vapor pressure formulation for water in range 0 to 100°C: A revision. *J. Res. Nat. Bur. Stand.*, **80A**, 775–785.
- Willet, K. M., Jones, P. D., Gillett, N. P., Thorne, P. W. (2008). Recent changes in surface humidity: Development of the HadCRUH dataset. *J. Climate*, **21**, 5364–5383.

ACKNOWLEDGEMENTS

I owe a debt of gratitude to many people whose help has been crucial to my success in completing this dissertation. First of all, I have been privileged to have the direction of two supervisors, Assoc. Prof. Hanno Ohvril and PhD Erko Jakobson. Both of them have made invaluable contributions to the development of my ideas, have been generous with their time and provided helpful advice on the writing process.

I would like to express my gratitude to Anu Reinart from Tartu Observatory, who has provided the opportunity to begin with doctoral studies and guaranteed the financial support in various ways throughout the past four years.

I am very grateful to Kalev Rannat, who has been like a third supervisor for me. His assistance and advice have been enormously useful for studying GPS-meteorology as well as carrying out calculations at the High Performance Computing Center of the University of Tartu.

I would like to offer my sincere thanks to Holger Vömel and Larry Miloshevich for their comments and suggestions regarding the correction of radiosonde humidity measurements.

I am deeply thankful to Rüdiger Haas and Gunnar Elgered from Chalmers University of Technology for coming up with new research topics, and by this, motivating me to complete the dissertation in time.

I owe a great deal to my colleagues from the Laboratory of Atmospheric Physics.

I am deeply grateful to my parents for support and encouragement.

Finally, I would like to thank my family – Maria, Teresa, Agata and Lukas – for just being there for me and for inspiring me with infinite joy.

It would be difficult to acknowledge everyone who has in some way or another contributed to the research reported in this dissertation.

The doctoral studies were supported by a project “Estonian radiation climate” (European Regional Development Fund) and European Social Fund’s Doctoral Studies and Internationalisation Programme DoRa.

PUBLICATIONS

CURRICULUM VITAE

Name: Hannes Keernik
Date of birth: April 21, 1986
Citizenship: Estonian
E-mail: hannes.keernik@ut.ee
Phone: +372 5804 7724

Education:

2011–2015 University of Tartu, PhD studies in Environmental Physics;
2008–2011 University of Tartu, MSc in Environmental Monitoring Technology (“Column water vapour: intercomparison of its estimation techniques”);
2005–2008 University of Tartu, MSc in Environmental Monitoring Technology (“Column water vapour at Tõravere during 2002–2007”).

Lecture courses:

- Fundamentals of the Environmental Physics I, 3 ECTS, University of Tartu;
- Fundamentals of the Environmental Physics II, 3 ECTS, University of Tartu.

Employment:

2015–... Tartu Observatory, junior research fellow;
2011–2015 Tartu Observatory, engineer;
2006–... Estonian Environmental Research Centre, specialist.

Scientific and research activity:

Natural sciences and engineering, environmental physics – temporal and spatial variability of atmospheric water vapour.

Projects:

- Substitute member of the management committee of the COST Action ES1206 – “Advanced Global Navigation Satellite Systems tropospheric products for monitoring severe weather events and climate (GNSS4SWEC)”, 2013–date;
- Aerosols and greenhouse gases contribution to the climate change in the Baltic Sea region and in the Arctic (PUT645, E. Jakobson), 2015–date.

Visiting scholarships:

Institute for Space Sciences, Free University of Berlin (Germany): 17.03–21.03.2014. Host: prof Jürgen Fischer, retrieval of water vapour by satellites.

ELULOOKIRJELDUS

Nimi: Hannes Keernik
Sünniaeg: 21.04.1986
Kodakondsus: Eesti
E-post: hannes.keernik@ut.ee
Telefon: +372 5804 7724

Haridus:

2011–2015 Doktorantuur, Tartu Ülikool, Füüsika Instituut;
2008–2011 MSc keskkonnanafüüsikas (keskkonnaseire tehnoloogia), Tartu Ülikool: “Õhusamba niiskussisaldus – erinevate määramisviiside võrdlus”;
2005–2008 BSc keskkonnanafüüsikas, Tartu Ülikool: “Atmosfääri niiskussisaldus Tõraveres 2002–2007”.

Loengukursused:

- Keskkonnanafüüsika alusedI, 3 ECTS, Tartu Ülikool;
- Keskkonnanafüüsika alusedII, 3 ECTS, Tartu Ülikool.

Teenistuskäik:

2015–... Tartu Observatoorium, nooremteadur;
2011–2015 Tartu Observatoorium, insener;
2006–... Eesti Keskkonnauuringute Keskus, spetsialist.

Teadus- ja arendustegevus:

Loodusteadused ja tehnika – atmosfääri niiskussisalduse ruumiline ja ajaline muutlikkus.

Osalus projektides:

- Korralduskomitee asendusliige COST projektis ES1206 – “Advanced Global Navigation Satellite Systems tropospheric products for monitoring severe weather events and climate (GNSS4SWEC)”, 2013–...
- Aerosoolide ja kasvuhoonegaaside panus kliima muutusesse Läänemere regioonis ning Arktikas (PUT645, E. Jakobson), 2015–...

Täiendamine välismaal:

Kosmoseteaduse Instituut, Berliini Vaba Ülikool: 17.03–21.03.2014. Atmosfääri niiskussisalduse määramise satelliidimeetodid.

DISSERTATIONES GEOPHYSICALES UNIVERSITATIS TARTUENSIS

1. **Andres Kuusk.** The hot-spot effect in plant canopy reflectance. Tartu, 1991.
2. **Tiit Nilson.** Radiative transfer in non-homogeneous plant canopies. Tartu, 1991.
3. **Helgi Arst.** Atmosfääri ja mere kiirguskarakteristikud looduskeskkonna seisundi informaatoritena (vene keeles). Tartu, 1991.
4. **Juha Sarkkula.** Measuring and modelling water currents and quality as a part of decision making process for water pollution control. Tartu, 1992.
5. **Piia Post.** On the two radiatively effective cloud parameters. Tartu, 1993.
6. **Aadu Mirme.** Electric aerosol spectrometry. Tartu, 1994.
7. **Aare Luts.** Mathematical simulation of the evolutions of air ions. Tartu, 1995.
8. **Tiit Kutser.** Estimation of water quality in turbid inland and coastal waters by passive optical remote sensing. Tartu, 1997.
9. **Ülle Kikas.** Atmospheric aerosol in the Baltic region. Tartu, 1998.
10. **Tarmo Kõuts.** Processes of deep water renewal in the Baltic sea. Tartu, 1999.
11. **Anu Reinart.** Underwater light field characteristics in different types of Estonian and Finnish lakes. Tartu, 2000.
12. **Marko Kaasik.** Parameterisation of atmospheric boundary layer in the numerical model of air pollution transport. Tartu, 2000.
13. **Janek Laanearu.** Topographically constrained deep-water flows in channels. Tartu, 2001.
14. **Urmas Raudsepp.** Wind-driven circulation in the gulf of Riga. Tartu, 2001.
15. **Urmas Hõrrak.** Air ion mobility spectrum at a rural area. Tartu, 2001.
16. **Marko Vana.** Formation and evolution of atmospheric aerosol size spectrum by the occurrence of nucleation burst events in the atmospheric boundary layer; transport of the climatically active particulate air pollution. Tartu, 2002.
17. **Veljo Kimmel.** Analysis of methods of air quality assessment. Applications in Estonia. Tartu, 2002.
18. **Oleg Okulov.** Variability of atmospheric transparency and precipitable water in Estonia. Tartu, 2003.
19. **Aarne Männik.** Implementation and validation of the nonhydrostatic adiabatic core of the numerical weather prediction model hirlam. Tartu, 2003.
20. **Matti Mõttus.** Shortwave solar radiation field inside willow canopy. Tartu, 2004.
21. **Kalev Rannat.** Long weakly nonlinear waves in geophysical applications. Tartu, 2007.
22. **Rigel Kivi.** Observations of ozone, polar stratospheric cloud and water vapour profiles in the arctic. Tartu, 2007.

23. **Erko Jakobson.** Spatial and temporal variability of atmospheric column humidity. Tartu, 2009, 125 p.
24. **Sander Mirme.** Development of nanometer aerosol measurement technology. Tartu, 2011, 118 p.